AN ANOMALY IN GEOMAGNETIC VARIATIONS ON THE WEST COAST OF BRITISH COLUMBIA

by

ANTHONY LAMBERT

B.Sc., University of British Columbia, 1963

A THESIS SUBMITTED IN PARTIAL FULFILMENT OF THE REQUIREMENTS FOR THE DEGREE OF MASTER OF SCIENCE

in the Department

of

GEOPHYSICS

We accept this thesis as conforming to the required standard

THE UNIVERSITY OF BRITISH COLUMBIA

April, 1965

In presenting this thesis in partial fulfilment of the requirements for an advanced degree at the University of British Columbia, I agree that the Library shall make it freely available for reference and study. I further agree that permission for extensive copying of this thesis for scholarly purposes may be granted by the Head of my Department or by his representatives. It is understood that copying or publication of this thesis for financial gain shall not be allowed without my written permission.

Department of GEOPHYSICS

The University of British Columbia,
Vancouver 8, Canada

Date APRIL 9, 1965

ABSTRACT

Four portable magnetometer stations were set up at intervals of 80 - 100 kilometers along an east-west profile running from Tofino on the west coast of Vancouver Island to Abbotsford on the mainland in order to study the spatial dependence of the coastal anomaly. These were supplemented by records from the permanent Victoria Magnetic Observatory. The Tofino-Abbotsford chain extends and partly overlaps an earlier chain of stations set up to search for geomagnetic anomalies along an east-west profile from Lethbridge, Alberta to Vancouver, British Columbia. The coastal anomaly recorded at Tofino is observed exclusively in the vertical component, diminishing rapidly inland and reaching its maximum value when the inducing field changes in approximately an east-west direction with a frequency between one and two cycles per hour. The horizontal and vertical variations are in a ratio of two to one at the coast which is in agreement with induction ratios calculated at coastlines in Australia and California. The directional dependence and limited spatial extent of the anomaly indicate a rather shallow conductivity discontinuity, at most 100 kilometers deep, running approximately parallel to the continental shelfline. Since at the maximum response frequency the upper mantle beneath the ocean is largely shielded by the overlying wedge of sea water, the anomaly is thought to be mostly due to the conductivity contrast between the deep ocean and the continent. The diurnal geomagnetic variations

which pass through the surface layers virtually unattenuated show at least a twenty five percent enhancement in the vertical component from Abbotsford to Tofino. This anomaly perhaps reflects a change in upper mantle conductivity more accurately than does the higher frequency Tofino anomaly. At a still higher frequency of three cycles per hour where the Tofino anomaly is already reduced, there is a small anomaly in the vertical component at Westham Island on the east side of Georgia Strait which is completely absent at lower frequencies. The influence of a shallow body of sea water such as Georgia Strait is expected to be small. Hence this anomaly is probably due to a conductivity structure beneath the Strait in the crust or upper mantle.

ACKNOWLEDGEMENTS

I am pleased to acknowledge the invaluable assistance and welcome criticism given by Mr. Bernard Caner, Director of the Victoria Geomagnetic Observatory. I am also indebted to Professor J.A. Jacobs for his kind and patient supervision and to Dr. T. Watanabe who provided useful discussion and criticism of the theoretical part of this thesis. Many thanks go to Mr. D. Weichert who assisted with the data analysis and to others in the Department of Geophysics who gave help when it was needed. The work in this thesis was partially supported by the National Research Council.

TABLE OF CONTENTS

FIGURES

TABLES

APPENDICES

I INTRODUCTION

A Coastal Geomagnetic Anomalies

This thesis is concerned with an anomaly in the vertical component variations of the geomagnetic field which was examined with four portable Askania magnetometers set up along an east-west profile in the vicinity of the British Columbia coastline, together with records from the Victoria Magnetic Observatory. Similar vertical anomalies have been measured at coastlines in many parts of the world and seem to be correlated with the horizontal magnetic field variations in a direction approximately perpendicular to the coastline.

Parkinson(24) has analyzed a large number of magnetograms from coastal stations all over the world and finds that there is a strong tendency for the vectors representing changes in the geomagnetic field to lie on or close to a plane. At coastal stations this plane tilts upward towards the nearest deep ocean, the only exceptions being at a few stations where the structure of the continental shelf is complicated.

Similarly, Rikitake(41) and his co-workers have studied intensively the vertical anomaly in geomagnetic bays measured on the main Japanese Island and have found that it is best observed when the inducing field changes in a north-south direction approximately perpendicular to the shelfline south of the island.

Along the California coastline Schmucker(47) has recorded anomalously large vertical components (Z) in long period Sq

and short period bay type variations, together with slightly reduced horizontal variations (D,H) at the shorter periods. The vertical anomaly there is also correlated with horizontal changes perpendicular to the California coastline.

Other measurements in coastal regions have furnished interesting results. In perticular, Mason and Hill[20] found that the daily range of geomagnetic total force variations was conspicuously greater over the continental shelf in the north east Atlantic than at the shore by a factor of two. Off the west coast of Italy at Ponza Island (Simeon and Sposito[49]) there is a startling parallelism between the vertical and horizontal variations which is absent at stations in central Italy.

In the Arctic (Zhigalov[61]) measurements from an ice floe drifting across the continental shelf into deeper water showed vertical component variations of diminishing amplitude as the sea depth increased, especially for short period fluctuations, of the order of minutes.

At Mirny in the Antarctic Mansurov[19] has reported an increase in vertical component variations at the coastline and an increase in horizontal variations on the ice just seaward of the coastline. The ratio of vertical to horizontal variations on the land near the coast increased as the period decreased to the order of seconds. This result is consistent with the frequency dependence of this ratio at the coastal stations of Westham Island and Victoria in British Columbia (Christoffel, et al[10]).

B Possible Explanations of the Anomalies

All these coastal phenomena can be included under the general term "coast effect" and although some of them may be caused by localized subterranean distributions of conducting material, it has been suggested (Parkinson[23], Chapman and Whitehead[7], Rikitake and Yokayama[34], Rikitake[35]) that they could perhaps be accounted for by the anomalous magnetic fields produced by electric currents induced in the more conducting oceans.

Another possible and far more interesting explanation, as far as Upper Mantle studies are concerned, is that the "coast effect" is at least partly due to a lateral conductivity discontinuity in the crust and/or upper mantle at the boundary of continent and ocean. The Mohorovičić discontinuity dips

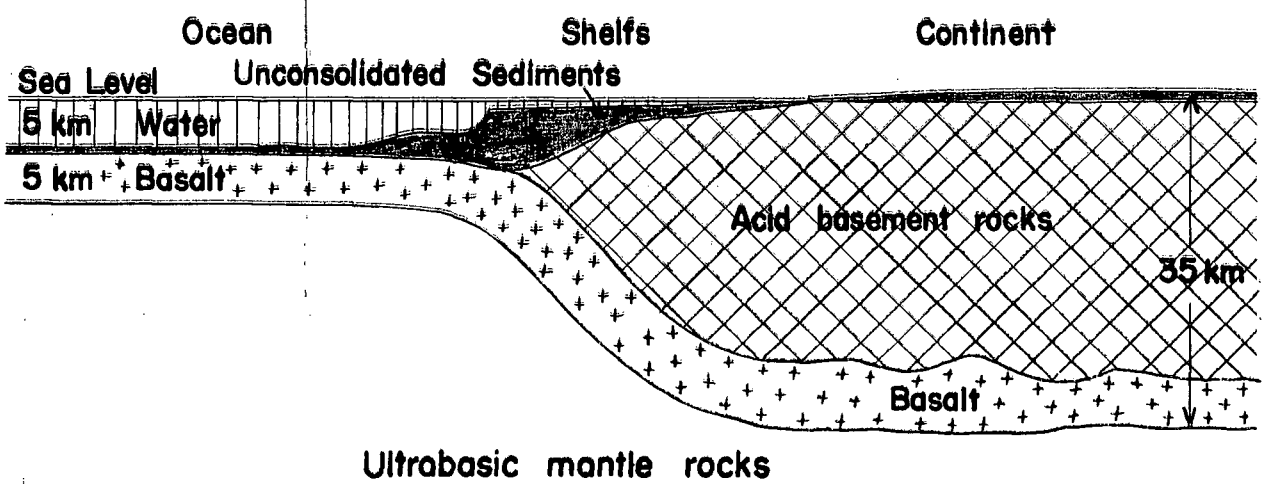

Figure 1. Generalized Section Across a Stable Continental Margin, after J.A. Jacobs, R.D. Russell, and J.T. Wilson.

sharply downward (Hess[15], Dietz[12]) as the transition is approached from ocean to continent, and according to heat flow

measurements, there is a marked difference between the constitution of the upper part of the mantle beneath the two regions (Jacobs[17]) so that a conductivity discontinuity is not unlikely. Furthermore, seismic studies show a decrease in shear velocity at shallower depths under the oceans than under the continents (Dorman, et al[13]). Such a decrease in velocity has been attributed by Gutenberg[14] to the effect of increasing temperatures on the elastic constants of the rocks. Hence, the isotherms in the mantle beneath the continents could very well rise closer to the surface on passing into the shallower oceanic mantle providing increased electrical conductivity due to ionic conduction at a shallower level and resulting in a lateral conductivity anomaly in the upper mantle as a possible source for the "coast effect".

By such arguments, Schmucker[47] has proposed that the vertical conductivity discontinuity which was found at a depth of the order of 100km under continental North America (Niblett, et al[22], Cantwell[4], Srivastava[50]) may be at much shallower depths under the oceans resulting in a large conductivity step in the upper mantle beneath the continental shelf line. This conductivity step might roughly parallel the upper boundary of the low velocity layer, although it is doubtful (Rikitake[38]) that the low velocity layer itself is an extensive highly conducting layer extending over large parts of the earth.

Studies of heat flow anomalies in the eastern Pacific (Von Herzen and Uyeda[53]) lend strong support to arguments

for the possible existence of high temperature thermal sources at relatively shallow depths beneath the oceans especially in orogenic zones. In fact, it has been proposed (Rikitake[35]) that a highly conducting loop which could be composed of high temperature material provides an explanation for the Japanese "coast effect" anomaly.

Although such proposals furnish plausible reasons for expecting a coastal anomaly which is independent of the mapped geology, it is still not clear whether the "coast effect" is due to eddy currents in the conducting oceans or due to the upper mantle conductivity structure at the coast. If it is a hybrid effect due to both the conductivity discontinuities of ocean and upper mantle then the ocean water effect would have to be eliminated in order to study the deeper conductivity anomaly.

C Electromagnetic Induction in the Earth

The distance from the earth's surface to the closed electric current systems, generally believed to be the cause of transient magnetic fields, is very small compared with the wavelength of the fields, so the magnetic induction field predominates over the radiation field and the geomagnetic fluctuations may be derived from a potential function. The potential can be expressed in a series of spherical harmonics and is found to consist of an external part and a part of internal origin. The internal field is assumed to be caused solely by induction in the earth by the external field (Chapman and Bartels[9]).

The strength and distribution of the induced earth currents must, therefore, depend on the conductivity distribution and also on the nature of the inducing field. Hence, in order to study the conductivity distribution within the earth, ideally, a separation of the transient surface fields into external and internal parts must be made. This should be over a large region comparable in extent to the entire earth's surface or over a region of more limited extent, depending on whether the average conductivity within the earth as a whole or local conductivity distributions are being considered. Different methods of separating the field over an area of the earth's surface small enough to be treated as plane, have been described by Siebert and Kertz[48], Schmucker[45] and Weaver[57]. Rikitake[40] has approximated the potentials of internal and external origin due to a magnetic disturbance by two pairs of radially opposed dipoles, one outside the Earth and one inside the Earth, in the region of the Asian continent.

D Theoretical Conductivity Models

Theoretical calculations have been carried out in attempts to correlate the behaviour of the time dependent part of the geomagnetic field over the earths surface with the conductivity distribution within the earth. Information about the electrical state of the earth can be obtained, as in this thesis, by an analysis, at a given frequency, of the relative amplitudes and phases of the three magnetic field components Z, H and D of the natural geomagnetic fluctuations over the region of interest, or

through an examination of the variation with frequency of the horizontal components of the natural time dependent magnetic and electric fields at a particular location on the earth's surface (Cagniard[3], Wait[54], Price[30]). So far, however, no success has been achieved in calculating the conductivity distribution directly from such information on the natural geomagnetic fluctuations. Rather, the distribution of conducting material is inferred by comparing the measured surface field with that calculated for an assumed model conductivity distribution often based on seismic, gravity and geological information.

The world wide average of the ratio of internal to external parts of the solar (Sq) and lunar (L) daily magnetic variations was found to be consistent with a spherically symmetric earth model consisting of a uniform "core" with conductivity 3.6×10^{-13}emu. surrounded by a non-conducting outer shell (Chapman[6], Chapman and Whitehead[7]). Later, the theory of induction in a conducting sphere was extended to a consideration of the internal and external parts of the magnetic storm time variations (D_{ST}). This, in turn, led to the treatment of an earth model in which the conductivity in the "core" varied as r^{-m} (Lahiri and Price[18]) (where r is the earth's radius and m an integer) in order that theoretical results might be compatible with both the observed daily variations and the storm time variations. The solution required a worldwide increase in conductivity at a depth of about

700 kilometers together with a surface conductivity distribution suggesting the influence of the highly conducting oceans. (Chapman and Whitehead[7], Lahiri and Price[18]). However, on the basis of more numerous and reliable data, new analyses of the amplitude ratio and phase difference between the external and internal parts suggest that the depth of the uniform conducting core should be at 400km with a conductivity of 5×10^{-12} emu. This new uniform core model overcomes the discrepancy between the induction field from Sq and D_{ST}. More localized analyses have revealed a large increase in conductivity at depths as shallow as 100 kilometers beneath the North American continent (Srivastava[50], Niblett[22], Cantwell[4]) and recent work in California (Schmucker[47]) suggests a more gradual transition from lower to higher conductivity values in order to explain the observed induction due to both long and short period variations. The practice of assuming a highly conducting core whose spherical surface exists at a certain depth below the earth's surface would, therefore, seem to be unrealistic, since the depth and rapidity of the major conductivity increase in the upper mantle appears to vary from place to place.

Using the theory of induction of electric currents in non-uniform thin sheets and shells (Price[28], Ashour[1]), Rikitake [36, 37] studied electromagnetic induction caused by daily variations in a hemispherical ocean underlain by a concentric sphere of uniform conductivity and also induction caused by geomagnetic bays in a semi cylindrical ocean. His analyses

and that of de Wett who considered the induction of electric currents in an ocean model represent the first attempts to approximate geomagnetic variations by considering a spherical earth model whose lateral surface conductivity variations resemble those of the earth's upper layers. Rikitake's solutions showed that electromagnetic coupling between the ocean and the conducting part of the earth's mantle reduced the expected anomaly in geomagnetic bays to a value less than forty percent of the inducing field and reduced the anomaly in the daily variations due to a hemispherical ocean to an almost negligable value. Recently, however, it has been shown (Roden[42]), on the basis of a flat ocean model, that in the case of daily variations, electric currents in the mantle can have but little effect in reducing the anomaly within distances from the edge of the ocean which are comparable to the depth at which the currents are flowing.

The problem of induction in a spherical earth model with complex boundary conditions near the surface is a prohibitive one and lately more interest has been shown in the interpretation of local anomalies involving simple theoretical model calculations in which the sphericity of the earth is neglected and the earth is treated as a semi-infinite plate conductor. The basic theory of the magnetotelluric method (Cagniard[3]) has been extended to the case where the earth contains a vertical discontinuity in conductivity. (d'Erceville and Kunetz[11], Rankin[32]). Because of its relevance to the

interpretation of the "coast effect" at micropulsation frequencies, this vertical fault problem has been studied further (Weaver[55], Coode[5]) in the light of criticisms of the theory of the magnetotelluric method (Wait[54], Price[30]) regarding the nature and distribution of the source field. However, no exact solution has been obtained. The California coastal anomaly of bay type disturbances has been treated theoretically as the result of a perturbation of the large-scale, uniform induction process in a horizontally stratified conductivity distribution (Schmucker[47]). A relaxation method developed by Price[28], taking into account the mutual induction between a conducting surface layer of varying thickness and a core of infinite conductivity, furnished a distribution of the anomaly which followed the observed data closely. In this theoretical model the anomalous vertical variations result from the edge of an oceanic current sheet at the surface and from currents flowing in the upper mantle beneath the continental surface layers. Similar theoretical calculations using conformal mapping methods, based on a model consisting of a large conductivity step close to the earth's surface, give a similar spatial distribution. Both of these models predict the observed increase in the anomaly as the frequency of the geomagnetic variations increases to the order of one cycle per hour.

E Experimental Conductivity Models

Theoretical investigations must involve vastly simplified conductivity distributions because of the extreme difficulty in solving induction problems with highly complex boundary conditions.

On the other hand, coastline and subsurface irregularities may be taken into account to some extent in laboratory model studies. In particular, experimental proof was obtained for the enhancement of vertical geomagnetic variations at the edge of a hemispherical ocean, and the anomalous effects of a conducting loop beneath Japan were investigated experimentally. (Nagata, et al[21]). More recently experiments performed with a flat, copper sheet model of the Pacific Ocean in the neighbourhood of Japan (Roden[42]) have yielded a distribution of diurnal and semi diurnal fields which agree qualitatively with observations. In Australia (Parkinson[25]) experiments have been performed on an earth model in which the oceans are represented by sheets of copper bent to lie on the surface of a sphere and a uniform highly conducting core at a depth of 600 kilometers is simulated by a sphere of aluminium. The primary field is introduced by a coil of wire wound in the form of the current function thought to produce bays, and held outside the sphere in a position corresponding to the ionosphere. Preliminary results show that for bay type disturbances the copper oceans have an effect which agrees qualitatively with observations at the coastline, but the conductors modify the field much less than the conductors present in the earth. Measurements in the interior of the continent indicate that the uniform highly conducting core should be at a much shallower depth.

It would seem, then, that the oceans are responsible for at least part of the "coast effect" but no realistic ocean

model, mathematical or experimental, has yet been devised which gives a quantitative explanation for the anomaly at all frequencies.

II THEORY

A Natural Geomagnetic Variations

It is believed that transient geomagnetic variations are caused by the interaction of solar particles with the earth's magnetic field. Analysis of these variations, both periodic and irregular, at different points on the earth's surface provides a tool for the study of the electric state of the earth. Changes in the total magnetic force vector are usually measured continually in the form of the three components D, H and Z each of which is recorded on a magnetogram. All three components undergo smooth and regular variations with a period of approximately one day. These daily variations may be separated into the solar daily variation (S) which depends mainly on latitude and local time and the much smaller lunar daily variation (L). Storm and bay type disturbances are superimposed on these periodic variations and commence at almost the same instant at all points on the earth's surface. Bay type disturbances, which last for about one half to two hours, show up on magnetograms as a deviation from the normal periodic daily variation, gradually increasing to a maximum value and then decreasing smoothly back to the undisturbed level. Certain phases of weak magnetic storms provide useful features, although they are usually more irregular and less easily analyzed than bays.

1. Normal Variations

Geomagnetic variations may be represented by a time dependent disturbance vector F(t) with components D(t), H(t) and Z(t)

which, in general, are functions of position P and frequency ω. The disturbance vector consists of parts of both an internal and an external origin, i.e. we can write $\vec{F}(t) = \vec{F}_e(P,\omega) + \vec{F}_i(P,\omega)$. A common assumption is that the magnetic permeability μ is unity (cgs units) and that the internal part arises solely from induction by the external part in the conducting earth. If the conductivity distribution in the earth is horizontally stratified, the geomagnetic variations are said to be "normal" and

$$\vec{F}(t) = \vec{F}_n(t) = \vec{F}_{en}(P,\omega) + \vec{F}_{in}(P,\omega)$$

2. Anomalous Variations

Lateral conductivity inhomogeneities may result in a deformation of the internal current system responsible for the normal internal part $\vec{F}_{in}(P,\omega)$ giving rise to an anomalous internal component $\vec{F}_{ia}(P,\omega)$ which varies from station to station. For simple conductivity structures where mutual induction can be ignored the total internal part may then be written as

$$\vec{F}_i(P,\omega) = \vec{F}_{in}(P,\omega) + \vec{F}_{ia}(P,\omega)$$

and the total disturbance vector as

$$\vec{F}(t) = \vec{F}_{en}(P,\omega) + \vec{F}_{in}(P,\omega) + \vec{F}_{ia}(P,\omega) .$$

Induction analysis leads one to expect a correlation between the anomalous variations $\vec{F}_{ia}(P,\omega)$ and the total normal variations

$$\vec{F}_n(t) = \vec{F}_{en}(P,\omega) + \vec{F}_{in}(P,\omega) .$$

3. Separation of the Field into an Internal and an External Part

If the inducing field is essentially uniform, any differences

in geomagnetic variations observed at adjacent stations can be assumed to be due to an internal anomalous part. However, if the external inducing field is not uniform, the internal and external parts must be separated in order to determine the induced secondary fields associated with the conductivity anomaly. Assuming that the displacement current can be ignored, the magnetic variations may be derived from a potential function. The potentials due to internal and external electric currents may be represented as Fourier integrals involving spectral densities which decay exponentially with depth (see Induction Analysis, equation (22)) as follows:

$$\Omega_e(y,z) = -\int_0^\infty \left[\frac{e^{\lambda z} E_\lambda}{\lambda} \cos \lambda y + \frac{e^{\lambda z} F_\lambda}{\lambda} \sin \lambda y\right] d\lambda \quad , \quad \underline{z \geqslant 0}$$

$$\Omega_i(y,z) = -\int_0^\infty \left[\frac{e^{-\lambda z} e_\lambda}{\lambda} \cos \lambda y + \frac{e^{-\lambda z} f_\lambda}{\lambda} \sin \lambda y\right] d\lambda \quad , \quad \underline{z \geqslant 0}$$

where Z is measured vertically upward and Y in the direction of the total horizontal field variation H_T. The coefficients E_λ, F_λ, e_λ, f_λ are spectral densities and $2\pi/\lambda$ is the spatial wavelength. The field components at the earth's surface Z = 0 are given by

$$Z(y) = -\frac{\partial \Omega_e}{\partial z} - \frac{\partial \Omega_i}{\partial z} = \int_0^\infty \left[(E_\lambda - e_\lambda)\cos \lambda y + (F_\lambda - f_\lambda)\sin \lambda y\right] d\lambda$$

$$H_T(y) = -\frac{\partial \Omega_e}{\partial y} - \frac{\partial \Omega_i}{\partial y} = \int_0^\infty \left[(-E_\lambda - e_\lambda)\sin \lambda y + (F_\lambda + f_\lambda)\cos \lambda y\right] d\lambda$$

A Fourier Analysis can be carried out on the spatial dependence of the Z and H_T variations which are determined by measurement.

$$Z(y) = \int_0^\infty \left[A_z(\lambda)\cos\lambda y + B_z(\lambda)\sin\lambda y \right] d\lambda$$

$$H_T(y) = \int_0^\infty \left[A_{H_T}(\lambda)\cos\lambda y + B_{H_T}(\lambda)\sin\lambda y \right] d\lambda$$

The spectral densities $E_\lambda, F_\lambda, e_\lambda, f_\lambda$ in the expressions for the internal and external potentials may be found by equating the corresponding spectral densities in the expressions for $Z(y)$ and $H_T(y)$. Thus

$$A_z(\lambda) = E_\lambda - e_\lambda \qquad A_{H_T}(\lambda) = F_\lambda + f_\lambda$$

$$B_z(\lambda) = F_\lambda - f_\lambda \qquad B_{H_T}(\lambda) = -E_\lambda + e_\lambda$$

Hence, the internal and external contributions to the magnetic variations at the earth's surface may be calculated.

B Induction Analysis

The current system which is the source of the magnetic variations is assumed to vary periodically with time. All the field vectors contain a time factor $e^{i\omega t}$ and all time derivatives may thus be replaced by $i\omega$.

1. The General Theory of Induction

Using the electromagnetic system of units Maxwell's field equations are:

$$\text{div } \vec{E} = 4\pi\rho c^2 \qquad (1)$$

$$\text{div } \vec{H} = 0 \qquad (2)$$

$$\text{curl } \vec{H} = 4\pi K \vec{E} + \frac{1}{c^2}\frac{\partial \vec{E}}{\partial t} \qquad (3)$$

$$\text{curl } \vec{E} = -\frac{\partial \vec{H}}{\partial t} \qquad (4)$$

where the permeability μ is taken as unity everywhere, K is the conductivity of the medium, and ρ the charge density. These equations are applied to the regions above and within a semi infinite conductor which approximates conditions above and below the earth's surface.

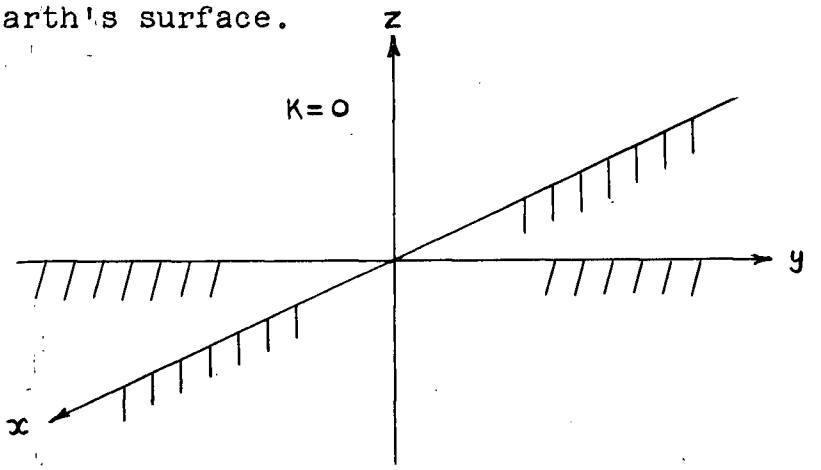

It is assumed that there is no space charge in the region above the conductor and that any charge distribution inside the conductor will be rapidly dispersed, so that we can write $\rho = 0$ everywhere and

$$\text{div } \vec{E} = 0 \qquad (5)$$

Taking the curl of equation (4) and combining it with equation (3) gives

$$\nabla^2 \vec{E} = i4\pi K\omega \vec{E} + \frac{(i\omega)^2}{c^2}\vec{E} \qquad (6)$$

For slowly varying fields and/or high conductivity $\frac{\omega^2}{c^2} << 4\pi K\omega$

Hence, inside the conductor equation (6) reduces to the diffusion equation

$$\nabla^2 \vec{E} = i 4\pi K \omega \vec{E} \qquad (7)$$

Above the conductor the conductivity K is negligible and the displacement term $\frac{\partial \vec{D}}{\partial t}$ can be neglected since the induction field dominates the radiation field in regions well within one wavelength of the source. Both terms on the right hand side of equation (6) can thus be neglected and in the region above the conductor, equation (6) reduces to Laplace's equation.

$$\nabla^2 \vec{E} = 0 \qquad (8)$$

With the above simplifications equation (3) becomes

$$\text{curl } \vec{H} = 0 \quad \text{and hence} \quad \vec{H} = -\text{ grad } \Omega$$

where Ω satisfies Laplace's equation since div $\vec{H} = 0$. Therefore, the magnetic field may be expressed as the gradient of a scalar potential in the region above the conductor.

The problem now is to find field vectors $\vec{E}$ and $\vec{H}$ which satisfy equations (5) and (7) inside the conductor, equation (8) above the conductor and the usual boundary conditions at the surface. Substituting $\vec{E} = Z(z)\,\vec{F}(x,y)\,e^{i\omega t}$ into equations (5), (7) and (8) yields

$$Z\left(\frac{\partial F_x}{\partial x} + \frac{\partial F_y}{\partial y}\right) + F_z \frac{\partial Z}{\partial z} = 0 \qquad (9)$$

$$\underline{z<0}, \quad \frac{\partial^2 \vec{F}}{\partial x^2} + \frac{\partial^2 \vec{F}}{\partial y^2} = \frac{1}{Z}\left[-\frac{\partial^2 Z}{\partial z^2} + i 4\pi K \omega Z\right]\vec{F} \qquad (10)$$

$$\underline{z>0}, \quad \frac{\partial^2 \vec{F}}{\partial x^2} + \frac{\partial^2 \vec{F}}{\partial y^2} = -\frac{1}{Z}\frac{\partial^2 Z}{\partial z^2}\vec{F} \tag{11}$$

The Form of Z(z) Above and Within the Conductor

The coefficients of $\vec{F}$ on the right hand side of equations (10) and (11) must be constant, since the left hand sides contain no Z dependence. Therefore let

$$\underline{z>0}, \quad -\frac{1}{Z}\frac{\partial^2 Z}{\partial z^2} = -\lambda^2 \tag{12}$$

and

$$\underline{z<0}, \quad -\frac{1}{Z}\frac{\partial^2 Z}{\partial z^2} + i4\pi\kappa\omega = -\lambda^2 \tag{13}$$

Solutions of equations (12) and (13) are:

$$\underline{z>0}, \quad Z = A e^{\lambda z} + B e^{-\lambda z} \tag{14}$$

$$\underline{z<0}, \quad Z = a e^{\theta z} \tag{15}$$

where $\theta^2 = \lambda^2 + i4\pi\kappa\omega$

ie. $\theta = \frac{1}{\sqrt{2}}\left[\left\{(4\pi\kappa\omega)^2 + \lambda^4\right\}^{\frac{1}{2}} + \lambda^2\right]^{\frac{1}{2}} + \frac{i}{\sqrt{2}}\left[\left\{(4\pi\kappa\omega)^2 + \lambda^4\right\}^{\frac{1}{2}} - \lambda^2\right]^{\frac{1}{2}}$

The solution (15) satisfies the condition that $Z(z) \to 0$ as $z \to -\infty$.

The Form of $\vec{F}(x,y)$ Above and Within the Conductor

Equation (9) yields an expression for $\vec{F}(x,y)$ which holds above and within the conductor. Let $F_z = 0$ so that

$$\frac{\partial F_x}{\partial x} + \frac{\partial F_y}{\partial y} = 0$$

Then

$$\vec{F} = \left(\frac{\partial P}{\partial y}, -\frac{\partial P}{\partial x}, 0\right) \tag{16}$$

where by equations (10) and (11)

$$\frac{\partial^2 P}{\partial x^2} + \frac{\partial^2 P}{\partial y^2} + \lambda^2 P = 0 \tag{17}$$

The Form of $\vec{E}$ and $\vec{H}$ Above and Within the Conductor

Above the Conductor ($z > 0$):

From expressions (14) and (16)

$$\vec{E} = (A e^{\lambda z} + B e^{-\lambda z})\left(\frac{\partial P}{\partial y}, -\frac{\partial P}{\partial x}, 0\right) \tag{18}$$

Equation (4) gives an expression for the magnetic field $\vec{H}$ in terms of the electric field $\vec{E} = Z\left(\frac{\partial P}{\partial y}, -\frac{\partial P}{\partial x}, 0\right)$

Thus

$$-i\omega\vec{H} = \text{curl}\ Z\left(\frac{\partial P}{\partial y}, -\frac{\partial P}{\partial x}, 0\right)$$

$$= \left(\frac{\partial Z}{\partial z}\frac{\partial P}{\partial x}, \frac{\partial Z}{\partial z}\frac{\partial P}{\partial y}, -\left(\frac{\partial^2 P}{\partial x^2} + \frac{\partial^2 P}{\partial y^2}\right)Z\right)$$

By equation (17) this becomes

$$-i\omega\vec{H} = \left(\frac{\partial Z}{\partial z}\frac{\partial P}{\partial x}, \frac{\partial Z}{\partial z}\frac{\partial P}{\partial y}, \lambda^2 PZ\right)$$

and on using equation (14)

$$\vec{H} = -\frac{\lambda}{i\omega}\ \text{grad}\left[\left(A e^{\lambda z} - B e^{-\lambda z}\right) P(x,y)\right] \tag{19}$$

Within the Conductor ($z < 0$):

From expressions (15) and (16)

$$\vec{E} = a e^{\theta z}\left(\frac{\partial P}{\partial y}, -\frac{\partial P}{\partial x}, 0\right) \tag{20}$$

Once again equation (4) gives an expression for the magnetic field $\vec{H}$

$$\vec{H} = -\frac{1}{i\omega}\left(\theta a e^{\theta z}\frac{\partial P}{\partial x}, \theta a e^{\theta z}\frac{\partial P}{\partial y}, \lambda^2 P a e^{\theta z}\right) \qquad (21)$$

The Scalar Magnetic Potential

Above the conductor, $\vec{H}$ = - grad Ω and thus by comparison with expression (19)

$$\Omega = -\left(A e^{\lambda z} + B e^{-\lambda z}\right) P(x, y, \lambda) \qquad (22)$$

where

$$\frac{\lambda A}{i\omega} = -A \quad \text{and} \quad \frac{\lambda B}{i\omega} = B$$

The term involving $A e^{\lambda z}$ corresponds to the field due to sources in the region above the conductor, whereas the term involving $B e^{-\lambda z}$ corresponds to the field of the induced currents inside the conductor.

Boundary Conditions

The tangential components of $\vec{E}$ and $\vec{H}$ are continuous at Z = 0. Thus, the tangential components of $\vec{E}$ given by equations (18) and (20) and the tangential components of $\vec{H}$ given by equations (19) and (21) may be equated at Z = 0 giving

$$A + B = a \qquad (23)$$

and

$$\lambda(A - B) = \theta a \qquad (24)$$

Written in terms of the coefficients A and B these yield

$$-i\omega(A - B) = \lambda a \qquad (25)$$

$$-i\omega(A + B) = \theta a \qquad (26)$$

Combining these expressions gives the value of B in terms of A, viz

$$B = \left(\frac{\theta - \lambda}{\theta + \lambda}\right) A \qquad \text{where} \qquad \theta^2 = \lambda^2 + i 4\pi K\omega .$$

Thus, the boundary conditions at the earth's surface require an image source beneath the surface with a strength depending on the conductivity K of the earth, the frequency of the variations ω and the spatial wavelength $2\pi/\lambda$.

2. Induction by a Periodic Linear Current in an Infinitely Conducting Half Space.

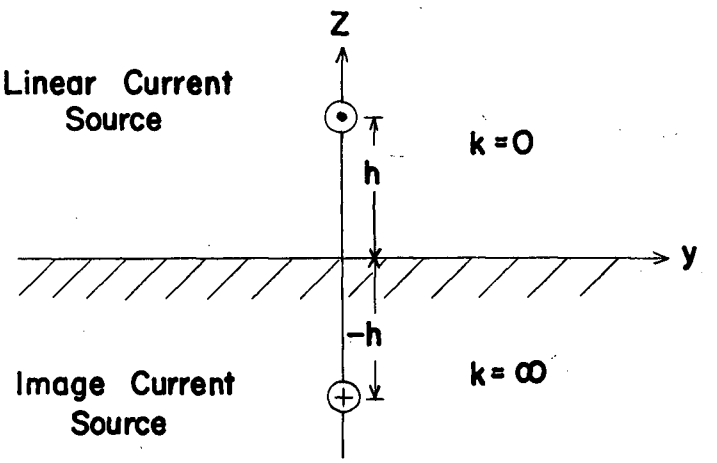

Consider a periodic current $I e^{i\omega t}$ flowing parallel to the x-axis in a positive direction at a height h above the earth's surface. The magnetic potential of this line current is given by $\Omega_e = 2 I e^{i\omega t} \tan^{-1}\left[\frac{h-z}{y}\right]$, which may be represented by Fourier's integral theorem as

$$\Omega_e = 2 \int_0^\infty I e^{i\omega t} e^{\lambda(z-h)} \sin \lambda y \, \frac{d\lambda}{\lambda} , \qquad 0 \leq z \leq h$$

The potential of the induced field arises from an image source

with strength $\left(\frac{\theta-\lambda}{\theta+\lambda}\right) I$, and thus the potential due to internal currents may be represented by

$$\Omega_i = 2 \int_0^\infty \left(\frac{\theta-\lambda}{\theta+\lambda}\right) I\, e^{i\omega t}\, e^{\lambda(-z-h)} \sin \lambda y \; \frac{d\lambda}{\lambda}$$

In the case of an infinitely conducting half space $\frac{\theta-\lambda}{\theta+\lambda}$ becomes unity and the image current source appears as a line current of strength I at a depth -h flowing in the opposite direction to the external source. The mirror image approximation may also be applied in the case of a finitely conducting horizontally stratified earth so long as high frequency variations are considered so that θ is very large and $\frac{\theta-\lambda}{\theta+\lambda}$ once again approaches unity. The external and induced vertical variations at the surface are:

$$Z_e(z=o) = -\frac{\partial \Omega_e}{\partial z}(z=o) = -2 \int_0^\infty I\, e^{i\omega t}\, e^{-\lambda h} \sin \lambda y \; d\lambda$$

and

$$Z_i(z=o) = -\frac{\partial \Omega_i}{\partial z}(z=o) = 2 \int_0^\infty I\, e^{i\omega t}\, e^{-\lambda h} \sin \lambda y \; d\lambda$$

Therefore $Z_e = -Z_i$ at Z = 0 and the total vertical variation is zero at the surface of an infinitely conducting half-space. The external and induced horizontal variations at the surface are:

$$H_{ey}(z=o) = -\frac{\partial \Omega_e}{\partial y}(z=o) = -2 \int_0^\infty I\, e^{i\omega t}\, e^{-\lambda h} \cos \lambda y \; d\lambda$$

and

$$H_{iy}(z=0) = -\frac{\partial \Omega_i}{\partial y}(z=0) = -2\int_0^\infty I\, e^{i\omega t}\, e^{-\lambda h} \cos \lambda y \, d\lambda$$

Therefore $H_{ey} = H_{iy}$ at Z = 0 and the total horizontal variation is $2H_{ey}$ at the surface. In reality, the conductivity of the earth is finite and in the case of longer period bay type disturbances, the image source will be weaker than a mirror image, the vertical component will not be completely cancelled and the horizontal component will be increased less than two-fold.

C The Effect of an Ocean on Geomagnetic Variations

The boundary between ocean and continent represents an obvious lateral conductivity discontinuity which will be responsible for an anomalous internal magnetic field. The anomaly may be studied as the edge effect of a large scale system of eddy currents induced in a thin sheet of uniform conductivity representing the ocean. Since the depth of a large ocean is negligably small compared to its horizontal dimensions, the currents would be expected to circulate in large eddies flowing parallel to the ocean floor.

1. Relation between Electric Currents and Magnetic Fields in a Thin Uniformly Conducting sheet

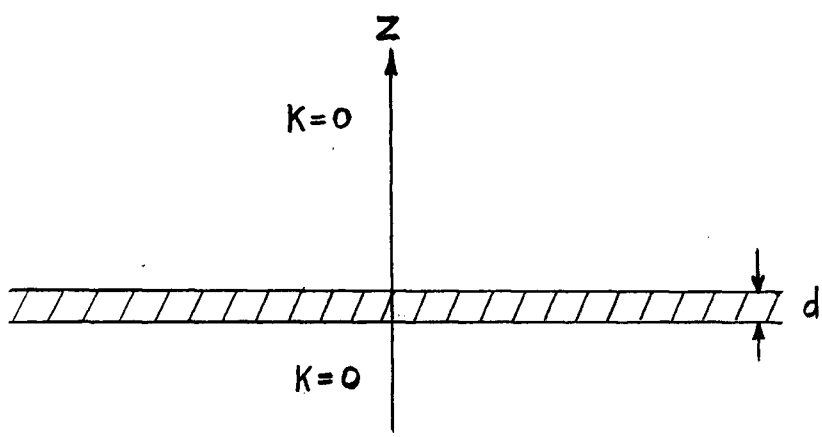

Neglecting the displacement current as in part B, the relevant field equations are:

$$\text{curl } \vec{H} = 4\pi \vec{i} \tag{1}$$

$$\text{curl } \vec{E} = -\frac{\partial \vec{H}}{\partial t} \tag{2}$$

$$\text{div } \vec{H} = 0 \tag{3}$$

$$\vec{i} = K\vec{E} \tag{4}$$

where the permeability μ is taken as unity (cgs units) and K is the conductivity of the thin sheet.

Above and below the sheet $\vec{i} = 0$, so that curl $\vec{H}$ = 0 and hence $\vec{H}$ = - grad Ω (5)

where Ω satisfies Laplace's equation. If the thickness of the sheet is infinitesimal, the currents will flow parallel to the surface of the sheet and the normal component $\vec{H}_n$ of the magnetic field and the tangential component $\vec{E}_t$ of the electric field have the same magnitude and direction on both sides of the sheet. Integrating equation (4) over the thickness of the sheet

$$\int_0^d \vec{i}\, dz = \int_0^d K\vec{E}\, dz = \vec{E}_t \int_0^d K\, dz$$

ie. $$\vec{i}_t = \vec{E}_t \sigma \tag{6}$$

where $\vec{i}_t = \int_0^d \vec{i}\, dz$ and $\sigma = \int_0^d K\, dz$ are the total sheet current intensity per unit length at a point on the surface and the total conductivity per unit length. Applying equation (1) to a small volume element enclosing part of the thin sheet,

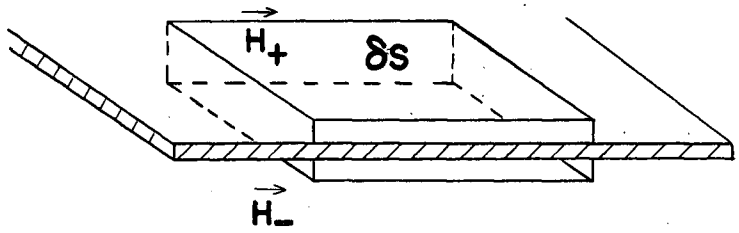

$$\iiint \operatorname{curl} \vec{H}\, dV = \iiint 4\pi \vec{i}\, dV \qquad (7)$$

using the identity $\iiint \operatorname{curl} \vec{a}\, dV = \iint \vec{n} \times \vec{a}\, dS$

and the definition of total sheet current intensity per unit length, equation (7) reduces to

$$\iint \vec{n} \times \vec{H}\, dS = \iint 4\pi \vec{i}_t\, dS^+$$

By shrinking the volume while still enclosing the sheet, we can write

$$\vec{n} \times (\vec{H}_+ - \vec{H}_-)\, \delta S = 4\pi \vec{i}_t\, \delta S$$

ie. $$\vec{i}_t = \frac{1}{4\pi} \vec{n} \times (\vec{H}_+ - \vec{H}_-) \qquad (8)$$

where $\vec{n}$ is the unit vector in the positive Z direction, $\vec{H}_+$ is the total field above the sheet and $\vec{H}_-$ the field below.

Applying equation (2) to a small circuit in the surface of the sheet at Z = 0, gives

$$\operatorname{curl} \vec{E}_t = -\frac{\partial \vec{H}}{\partial t}$$

which together with equations (6) and (8) yields

$$\text{curl}\left[\vec{n}\times(\vec{H}_+-\vec{H}_-)\right] = -4\pi\sigma\frac{\partial\vec{H}}{\partial t}$$

Taking the scalar product of both sides of this equation with $\vec{n}$, we obtain the boundary equation

$$\text{div}\,(\vec{H}_+-\vec{H}_-) = -4\pi\sigma\frac{\partial H_z}{\partial t} \qquad (9)$$

Now $$\vec{H}_+-\vec{H}_- = -\text{grad}\,(\Omega_+-\Omega_-)$$

and $\Omega=\Omega^e+\Omega^i$, where Ω^e and Ω^i are the magnetic potentials of internal and external origin. Since $\Omega^e_+ \cong \Omega^e_-$ we have:

$$\vec{H}_+-\vec{H}_- = -\text{grad}\,(\Omega^i_+-\Omega^i_-) \qquad (10)$$

The magnetic potential of the induced currents in a sheet at Z = o will have the same distribution on both sides of the sheet, the potentials on one side being the negative of the potentials on the other.

ie. $$\Omega^i_+(x,y,z) = -\Omega^i_-(x,y,-z)$$

so that at Z = 0 $$\Omega^i_+ = -\Omega^i_-$$

and $$\frac{\partial\Omega^i_+}{\partial z} = \frac{\partial\Omega^i_-}{\partial z}$$

Therefore equation (10) becomes

$$\vec{H}_+-\vec{H}_- = -2\left(\underline{i}\frac{\partial\Omega^i_+}{\partial x}+\underline{j}\frac{\partial\Omega^i_+}{\partial y}\right) \qquad (11)$$

where $\underline{i}$ and $\underline{j}$ are unit vectors in the x and y directions.

Substituting this into equation (9) together with $H_z = -\frac{\partial \Omega_+^e}{\partial z} - \frac{\partial \Omega_+^i}{\partial z}$ we obtain

$$-\left[\frac{\partial^2 \Omega_+^i}{\partial x^2} + \frac{\partial^2 \Omega_+^i}{\partial y^2}\right] = 2\pi\sigma \frac{\partial}{\partial t}\left[\frac{\partial \Omega_+^e}{\partial z} + \frac{\partial \Omega_+^i}{\partial z}\right]$$

and since Ω_+^i must satisfy Laplace's equation, this boundary equation becomes

$$\frac{\partial^2 \Omega_+^i}{\partial z^2} = 2\pi\sigma \frac{\partial}{\partial t}\left[\frac{\partial \Omega_+^e}{\partial z} + \frac{\partial \Omega_+^i}{\partial z}\right] \qquad (12)$$

Let the inducing potential field be of the form

$$\Omega^e = e^{\lambda z} e^{i\omega t} P(x,y)$$

Then the induced field above the sheet will be of the form

$$\Omega_+^i = k\, e^{-\lambda z} e^{i\omega t} P(x,y) \qquad (13)$$

so that $\Omega^e \to 0$ as $z \to -\infty$

and $\Omega_+^i \to 0$ as $z \to +\infty$

By substituting Ω^e and Ω_+^i into the boundary equation (12),

$$k = \frac{2\pi\sigma i\omega}{\lambda + 2\pi\sigma i\omega}$$

The modulus of k gives the ratio of the magnitudes of Ω_+^i and Ω^e and the argument of k gives the phase shift of the induced field relative to the inducing field. The electric current intensity per unit length $\vec{i}_t$ in the sheet can now be expressed in terms of the inducing field $\vec{H}^e$. Substituting equation (13) into (11) we have

$$\vec{H}_+ - \vec{H}_- = -2k\left(\underline{i}\frac{\partial \Omega^e}{\partial x} + \underline{j}\frac{\partial \Omega^e}{\partial y}\right)$$

which in turn may be substituted into equation (8) to give

$$\vec{i}_t = \frac{k}{2\pi} \vec{n} \times \vec{H}^e_t \qquad (14)$$

The electric current per unit length at a point in the sheet is, therefore, linearly correlated with the component of the external inducing magnetic field variation perpendicular to it.

2. The Edge Effect of a Current Sheet

Neglecting the effect of the ocean boundary in modifying the electric currents, and treating the current sheet as uniform right up to the edge, provides a simplified picture of the spatial distribution of the associated vertical magnetic fields. Mutual induction between the current sheet and any conductivity distribution beneath it is also neglected.

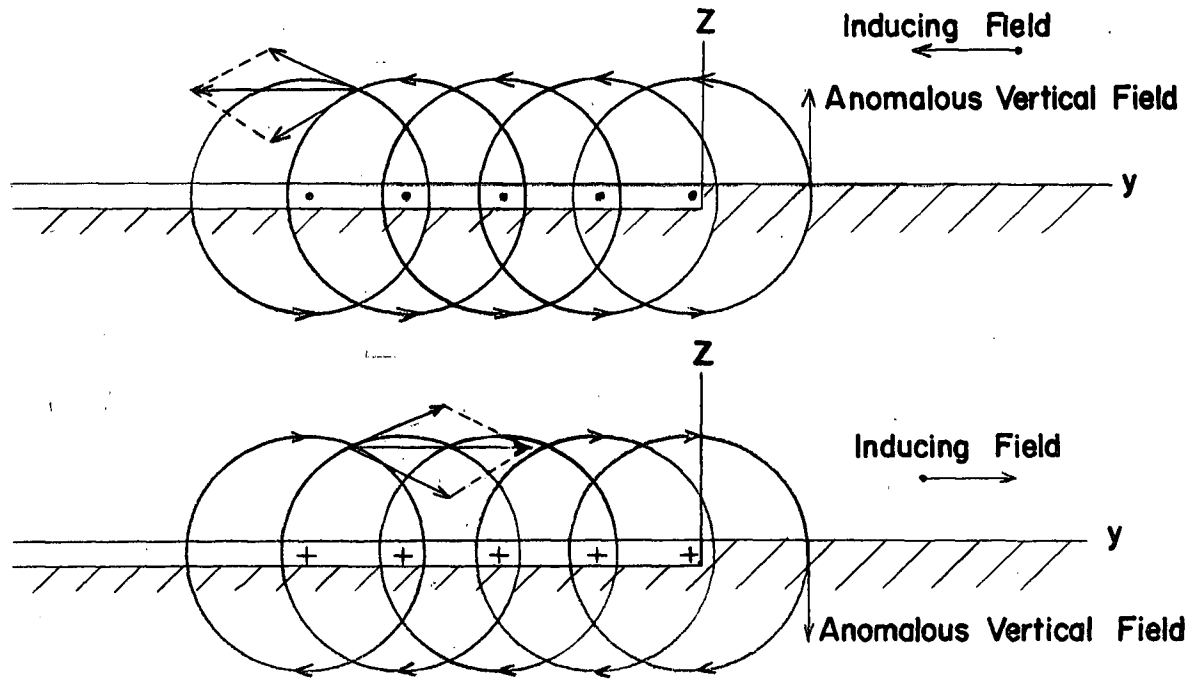

Figure 2 Electric Currents and their Associated Magnetic Fields at the Edge of a Uniformly Conducting Sheet.

The vertical magnetic field at a point (y,z) due to a line current of infinite length in a direction perpendicular to the y-axis and of strength $i_t\, dy'$ situated at a point (y',0) is given by

$$H_z = 2\, i_t\, dy' \left[\frac{y-y'}{z^2+(y-y')^2} \right]$$

The effect of a current sheet of infinite length, extending from y = 0 to y = -W, may be approximated by integrating the vertical fields contributed by a number of such line currents perpendicular to the y-axis and in the plane of the thin conductor.

Hence, the vertical field due to the sheet is given by

$$H_z = \int_0^{-W} \frac{2(y-y')\, i_t\, dy'}{z^2+(y-y')^2} = i_t \log \left[\frac{z^2+y^2}{z^2+(y+W)^2} \right] .$$

i.e.

$$H_z = \frac{k H_y^e}{2\pi} \log \left[\frac{z^2+y^2}{z^2+(y+W)^2} \right]$$ using equation (14)

This expression gives the expected spatial dependence and directional dependence of the vertical, edge-effect, anomaly, viz

1) The vertical anomaly increases as the ocean is approached, reaching a maximum at the coastline.

2) The anomaly is linearly correlated with the horizontal inducing field perpendicular to the coastline.

When the field changes toward the ocean the anomalous vertical change is positive (upward), and when the field changes toward the land the anomalous vertical change is negative

(downward). The expression for H_z is indeterminate at $z = 0$, $y = 0$ because of the mathematical nature of the model.

3. The Free Decay of Electric Currents in the Oceans

If the electric currents are excited in an ocean and left to decay, they will do so exponentially with a time constant which depends on the total conductivity of the ocean. The theory of electric currents in a uniformly conducting disc (Ashour[1]) shows that the time τ required for the current density to be reduced to $1/e$ of its initial value is given by $\tau = 2.34\, a/\rho$ where a is the radius of the disc and ρ is the surface resistance per unit length. Taking the conductivity K of sea water to be 4×10^{-11} emu, the radius of the Pacific Ocean 4000km., and the average depth 4 km., the above formula gives a free decay time of approximately four or five hours. Although bottom irregularities may reduce this decay time to a smaller value, it is evident that the Pacific Ocean will sustain electric currents induced by bay type disturbances of one or two hours duration. A curcular eddy current in the relatively shallow Georgia Strait between Vancouver Island and the mainland would decay in just a few seconds, so that in this case a vertical anomaly caused solely by the sea water is impossible for variations with a period greater than a few minutes.

4. The Shielding Effect of an Oceanic Layer

The magnetic fields of the induced currents in an ocean tend to cancel the source field beneath the layer. It has been shown in section C1 that the inducing and induced fields above

a thin conducting sheet are related by the following equation

$$\Omega_+^i(z) = k\,\Omega^e(-z)$$

where

$$k = \frac{2\pi\sigma i\omega}{\lambda + 2\pi\sigma i\omega}$$

Also

$$\Omega_+^i(z) = -\Omega_-^i(-z)$$

so that below the sheet the field is given by $\Omega_-^i = -k\,\Omega^e$

and the total field there is:

$$\Omega_- = \Omega^e + \Omega_-^i = (1-k)\,\Omega^e$$

Hence

$$\Omega_- = \left(\frac{\lambda^2 - i\,\lambda\,2\pi\sigma\omega}{\lambda^2 + 4\pi^2\sigma^2\omega^2}\right)\Omega^e$$

and the amplitude of the field variations below the sheet is reduced to a fraction

$$\frac{\lambda}{\sqrt{\lambda^2 + 4\pi^2\sigma^2\omega^2}}$$

of the external field. It is reasonable to suppose that spherical harmonics up to the tenth degree are sufficient to describe the field of a bay type disturbance in mid latitudes. Hence one can set an upper limit on the value of λ and a corresponding lower limit on the attenuation of the external field as it passes through a layer of ocean, three kilometers thick, in the vicinity of Vancouver Island. Setting the spatial wavelength $2\pi/\lambda$ equal to $2\pi R/10$ where R is the earth's radius gives $\lambda \simeq 1.6 \times 10^{-8}\ cm^{-1}$ Assuming that the conductivity K of sea water is 4×10^{-11}emu, the corresponding harmonic of the incident field will be reduced beneath the oceanic layer to ten percent of its value above the

ocean, for variations with a period of forty-five minutes. This calculation is, however, unrealistic in that it neglects the effect of a possible highly conducting region in the upper mantle beneath the ocean. Also, we are not entirely justified in assuming that the source of the magnetic variations is a stationary electric current system varying periodically with time, since there is now reason to believe (Rostoker, private communication) that the system is quite likely to drift relative to the earth's surface giving the source field a travelling wave nature.

5. The Effect of the Conducting Mantle on Electric Currents in the Oceans

There is a rapid increase in electrical conductivity in the vicinity of the upper mantle which may be represented theoretically by a highly conducting core in the earth's interior. Electric currents which are induced there are responsible for magnetic fields which suppress the induction of currents in the surface layers. Therefore, if the conducting region begins at a shallow depth, as might be expected beneath the oceans, mutual induction will reduce both the intensity of the oceanic current sheet and its shielding effect on the layers below.

III EXPERIMENTAL PROCEDURE

A Askania Variographs

The Askania variograph is a portable instrument consisting of three variometer units for recording the declination D, the horizontal intensity H and the vertical intensity Z, and a device for recording time marks, the temperature and a base line. The instrument is housed in a heat insulated case and a heater and thermostat are provided to keep the inside temperature at a constant level. The suspension fibres carrying the magnet systems can all be adjusted for complete temperature compensation, in case temperature fluctuations are permitted by the thermostat. Scale values for the three systems are determined by passing a known current through Helmholtz coils mounted on each variometer and noting the deflection. Movements of the systems are recorded by an optical system on photographic paper which is advanced by a 50c/s synchronous motor drive. The drive operated poorly on 60 cycle line power, causing a number of records to be lost. The recording magazine holds a ten meter roll of photographic recording paper which lasts for about twenty days operating at a speed of 24m.m./hour.

B Installation and Maintenance of the Variographs

The instruments, with the exception of the Westham Island variograph, were located indoors in reasonably non-magnetic buildings where 60 cycle, 110-115 volt power was available. The Tofino and Abbotsford stations were operated with the

assistance of the Department of Transport personnel and the Franklin River station was housed in a building provided by the courtesy of the MacMillan, Bloedel and Powell River Company. The instrument on Westham Island was located in a plywood shelter at the R.C.A.F. telemetry station. All the sites were checked with a portable Barringer 6M-102 proton precession magnetometer, and only those with low spatial gradients (< 5 γ per meter) were used.

The chronometers which provided the hourly time marks were set within a few seconds by W.W.V. short wave time signals. Records were also kept of the gain and loss of each chronometer so that corrections could be applied to the time marks in the event of an error greater than one minute. A calibration check of all three components was carried out for each roll of photographic film used in the variographs.

C Confidence Limits

The Helmholtz coil factors used in the calibration of the instruments are accurate to ±1%. The magnetometer deflection caused by calibrating currents can be measured to within about ±0.3m.m., i.e. about ±1% of the deflection. Unknown factors include: the meter calibration (probably better than ±1%); non-linearities in deflection of the order of 1% over the range of the magnetogram; inaccurate meter reading under difficult field conditions (probably under 1%). The overall accuracy of magnetogram features should, therefore, be better than ±3 to 5%. For the purpose of this survey, the instrumental confidence

limits have been arbitrarily set at 5%, i.e. differences in amplitute recorded at different stations are considered (instrumentally) significant only if they exceed 5%.

D Processing of Records

The photographic recording paper in the variographs was changed approximately once every two weeks and developing was done using facilities at the Victoria Geomagnetic Observatory. Data for the Fourier Analysis of bays was obtained from the records (as shown below) by marking off each of the three components at 2.5 minute intervals and digitizing by means of a template.

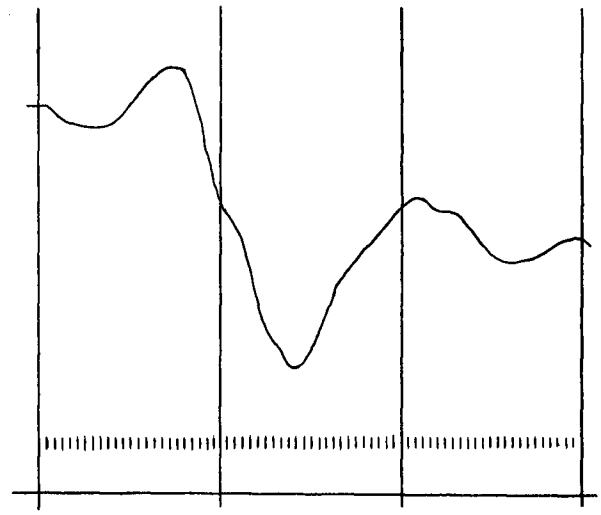

This spacing allows the calculation of Fourier coefficients for frequencies up to six cycles per hour. Daily variations were analyzed by digitizing the records at twenty minute intervals.

IV METHOD OF ANALYSIS

A Fourier Analysis

The analysis is based on the calculation of the spectral densities of each of the three components D,H, Z of a particular magnetic disturbance. A digital computer program based on Simpson's interpolation rule furnished the Fourier components for each of several bay type magnetic disturbances for frequencies from .001 cycles per minute to .061 cycles per minute. Ideally, a spectral analysis allows each of the three time dependent components D, H, Z of a disturbance to be expressed as a sum of simple harmonic time functions

$$f(t) = \int_{-\infty}^{+\infty} A(\omega) \cos \omega t \, d\omega + \int_{-\infty}^{+\infty} B(\omega) \sin \omega t \, d\omega$$

where the frequency functions $B(\omega)$ and $A(\omega)$ are the sine and cosine spectral densities (defined in Appendix II). Since Maxwell's field equations are linear, each of the Fourier components

$$f_\omega(t) = A(\omega)\, d\omega \cos \omega t + B(\omega) d\omega \sin \omega t$$

or

$$f_\omega(t) = C(\omega)\, d\omega \cos(\omega t - \varepsilon_\omega)$$

where $C(\omega) = \sqrt{A(\omega)^2 + B(\omega)^2}$ and $\varepsilon_\omega = \tan^{-1} \frac{B(\omega)}{A(\omega)}$

may be treated separately as linearly polarized harmonic waves of frequency ω incident on the earth's surface, and then the principle of superposition applied. Henceforth, the sine and cosine spectral densities $B(\omega)$, $A(\omega)$ will be used in place of the Fourier coefficients $B(\omega)\, d\omega$, $A(\omega)\, d\omega$ and the amplitudes

of the harmonic waves. Therefore, the Fourier component (at a frequency ω) of the total magnetic disturbance at the earth's surface can be written as the vector sum of three orthogonal harmonic terms

$$\vec{F}_\omega(t) = \underline{i}\, C_z(\omega)\cos(\omega t - \varepsilon_z) + \underline{j}\, C_H(\omega)\cos(\omega t - \varepsilon_H) + \underline{k}\, C_D(\omega)\cos(\omega t - \varepsilon_D)$$

in the directions of the three geomagnetic components Z, H, D. The corresponding external inducing disturbance is an elliptically polarized harmonic oscillation of frequency ω in a plane parallel to the earth's surface, comprised of linear harmonic oscillations in the D and H directions.

For a two dimensional anomalous zone, the anomalous part of the vertical magnetic disturbance Z_A at the earth's surface is correlated with the component of the horizontal disturbance perpendicular to the strike of the zone, denoted by S.

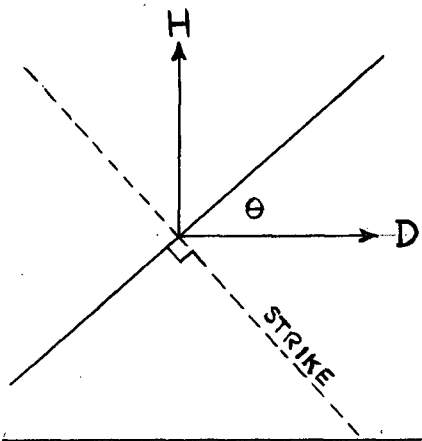

Thus
$$S = \sqrt{\left(B_D(\omega)\cos\theta + B_H(\omega)\sin\theta\right)^2 + \left(A_D(\omega)\cos\theta + A_H(\omega)\sin\theta\right)^2}$$

where
$$H_\omega(t) = A_H(\omega)\cos\omega t + B_H(\omega)\sin\omega t$$
$$D_\omega(t) = A_D(\omega)\cos\omega t + B_D(\omega)\sin\omega t$$

The linear horizontal disturbance S consists of parts of both external and internal origin and may itself contain an anomalous part varying with distance from the anomalous zone. If the assumption of two dimensionality is not justified, the approximate magnitude of the horizontal disturbance is given by

$$H_T = \sqrt{(C_H(\omega))^2 + (C_D(\omega))^2}$$

A study of the spatial dependence and frequency dependence of the quantities Z_A, S, Z_A/S and H_T permits a limiting estimate of the depth and extent of the conductivity anomaly.

B Polar Diagrams

Polar diagrams provide a means of testing a possible correlation between the vertical variations and the component of the horizontal variations in a particular direction (Parkinson[23]). The upper circle of the diagram is used to plot points corresponding to a change with an upward vertical component and the lower circle for a change with a downward vertical component. The points are plotted as in a Schmidt equal area projection, the radial distance of each point from the centre depending on the ratio of the vertical change to the horizontal change and the asimuthal angle ϕ of each point depending on the geographic direction of the horizontal change. A point at the centre of the diagram represents a change in the magnetic field in a vertical direction.

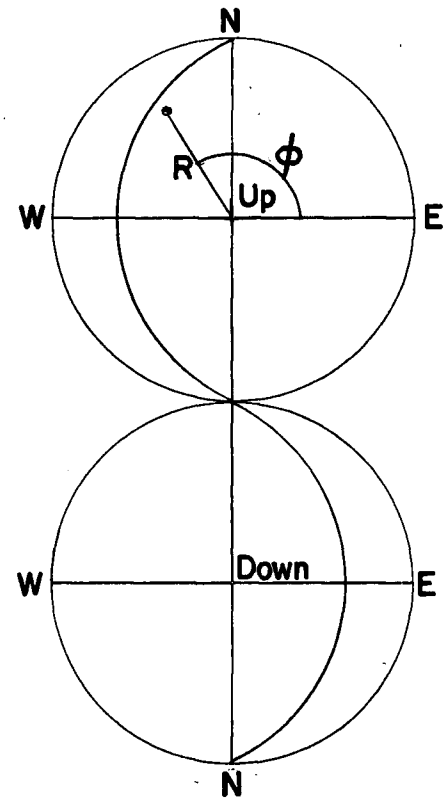

Figure 3 Method of Plotting a Polar Diagram

A Fourier Analysis breaks down a magnetic disturbance into in-phase and out-of-phase sinusoidal oscillations of the form

$$Z_\omega(t) = A_Z(\omega)\cos\omega t + B_Z(\omega)\sin\omega t$$

$$H_\omega(t) = A_H(\omega)\cos\omega t + B_H(\omega)\sin\omega t$$

$$D_\omega(t) = A_D(\omega)\cos\omega t + B_D(\omega)\sin\omega t$$

The horizontal change at a particular frequency ω can be regarded as the sum of two out of phase linear oscillations of the form

$$S_{\cos}(\omega) = \left(A_H(\omega) + A_D(\omega)\right)\cos\omega t$$

$$S_{\sin}(\omega) = \left(B_H(\omega) + B_D(\omega)\right)\sin\omega t$$

with asimuthal directions

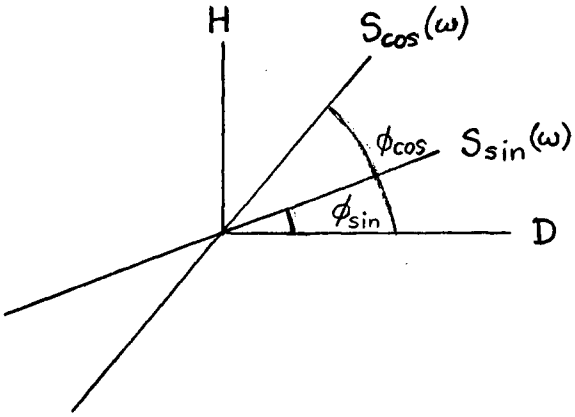

$$\phi_{cos} = \tan^{-1} \frac{A_H(\omega)}{A_D(\omega)},$$

$$\phi_{sin} = \tan^{-1} \frac{B_H(\omega)}{B_D(\omega)}$$

relative to the direction of D. When the conductivity is relatively large as it is in the oceans, it seems reasonable to assume that there is in-phase induction (Hyndman[16]), so that one is justified in attempting to correlate each of the horizontal linear oscillations $S_{cos}(\omega)$ and $S_{sin}(\omega)$ with the corresponding in-phase vertical oscillations $A_z(\omega)$ and $B_z(\omega)$ on a polar diagram. Hence, the Fourier analysis of one magnetic disturbance yields two points on the polar diagram defined by $A_z(\omega)$, $S_{cos}(\omega)$ and $B_z(\omega)$, $S_{sin}(\omega)$ corresponding to the frequency ω. If the anomalous zone is two dimensional, the points from the Fourier Analysis of a number of disturbances will be scattered along a great circle (Fig. 3) which will be symmetrical about the direction of best correlation, perpendicular to the strike of the anomalous zone. The correlation at each station can then be expressed by the induction coefficient C = Z/S. The scatter of the points which may vary with frequency will be enhanced if there is any out of phase induction and if the inducing wave contains too large an

uncompensated vertical component. In such cases, the directional dependence, indicated by the position of the great circle on the diagram, may become obscured and no induction coefficient can be defined for the station.

C Statistical Analysis

1. The Precision of a Mean Value

The mean value of a geomagnetic variable, such as Z, at a particular station can be estimated by sampling a number of geomagnetic disturbances. The precision of the mean value obtained from such a sample of n disturbances as an estimate of the long term mean value is given by the standard error S.E. = $\sigma/\sqrt{n}$ where σ is the standard deviation of a long series of observations. Using data from one sample, we can approximate σ by

$$\bar{\sigma} = \sqrt{\frac{\sum_i (z_i - \bar{z})^2}{n-1}}$$

so that the S.E. = $$\sqrt{\frac{\sum_i (z_i - \bar{z})^2}{n(n-1)}}$$

The probable error P.E. of a mean value is defined as the value of the deviation from the true long term mean which, in a normal distribution, will be exceeded on half the occasions

$$\text{P.E.} = 0.6745 \text{ (S.E.)}$$

$$= 0.6745 \sqrt{\frac{\sum_i (z_i - \bar{z})^2}{n(n-1)}}$$

The probable accuracy of all the mean values calculated in

this thesis are given in terms of the probable error P.E.

2. The Significance of a Mean Value

"Students" t test provides a method for testing whether a sample mean $\bar{Z}$ differs significantly from some postulated value Z', assuming that the long-term distribution of values of Z is nearly normal. The value of t is defined by $t = \frac{\bar{Z}-Z'}{S.E.}$ and "Student" has calculated the probability of exceeding any value of t derived from a random sample of n events. Adopting a confidence level of twenty percent requires that the calculated value of t be smaller than that value which has a one in five chance of occuring in any random sample; otherwise the data shows a significant deviation from the postulated mean value and a new mean value must be sought.

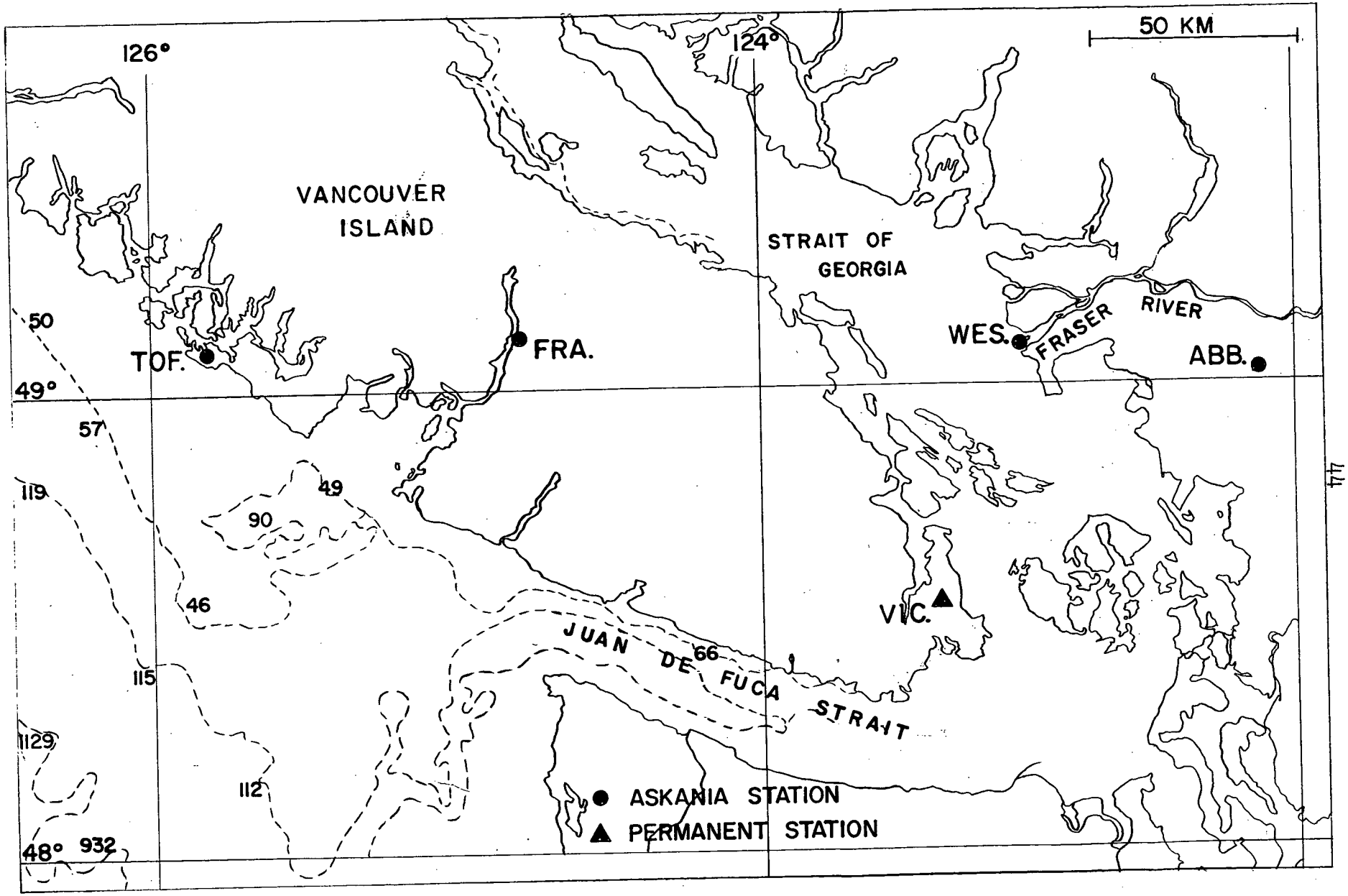

Figure 4. Location Map Showing Sites of Recording Stations

V RESULTS AND ANALYSIS

The sites of the stations used in the analysis are shown in Fig. 4. Tofino, Franklin River, Westham Island and Abbotsford were occupied by Askania variographs. Victoria is a permanent magnetic observatory. Two of these stations (Abbotsford and Westham Island) overlap the profile recorded by Hyndman[16]. Hyndman's analysis showed that the amplitude of the variations in both the horizontal and vertical components was essentially constant from Westham Island as far inland as Grand Forks (longtitude 118°30'). This means that Abbotsford and Westham Island can be used as representative inland stations.

A particular example of a geomagnetic disturbance, recorded simultaneously at Tofino and Victoria on Jan. 10th, 1964, is shown in Fig. 5 where the Z, H and D components have been redrawn to the same scale. A two to one enhancement in the vertical component at Tofino as compared to Victoria shows up clearly, whereas the H and D components are essentially identical. This disturbance was digitized at two and one half minute intervals and a Fourier analysis was carried out on the vertical component at the two stations. The sine and cosine spectral densities $B_z(\omega)$, $A_z(\omega)$ and the amplitude spectral densities $C_z(\omega)$ were plotted as a function of frequency showing a two to one enhancement of Tofino values over Victoria values covering virtually the entire frequency range from .001 cycles per minute to .061 cycles per minute (Figs. 6,7). A plot of the ratio $C_Z(\omega)_{TOFINO} / C_Z(\omega)_{VICT.}$ (Fig. 7) gives a better indication of the frequency dependence

of the Tofino anomaly and shows a peak at .036 cycles per minute (period ~ 30 min.) with another smaller peak at .053 cycles per minute (period ~ 20 min.).

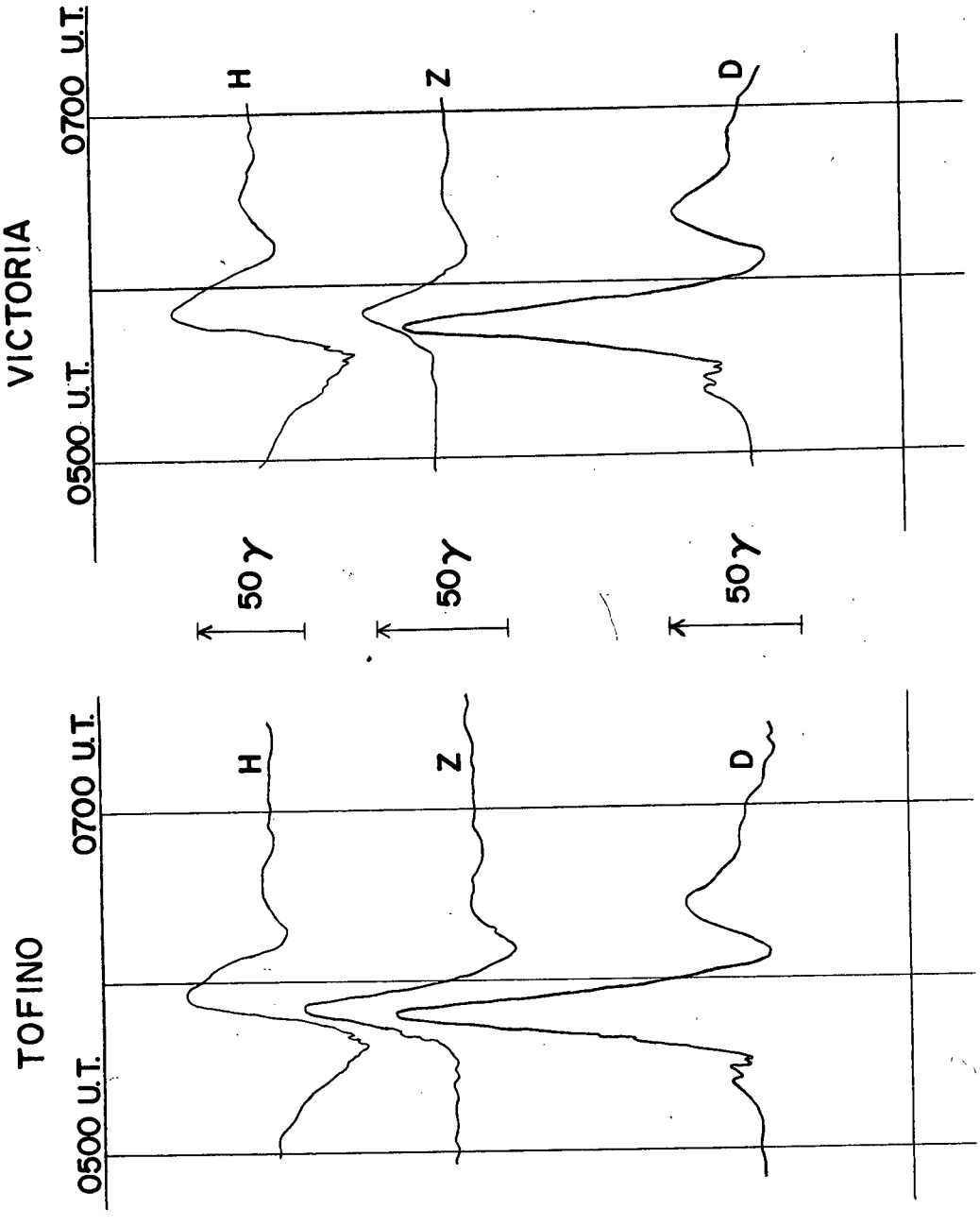

Figure 5. A Comparison of Magnetograms Showing an Enhancement in the Vertical Component at Tofino as Compared to Victoria

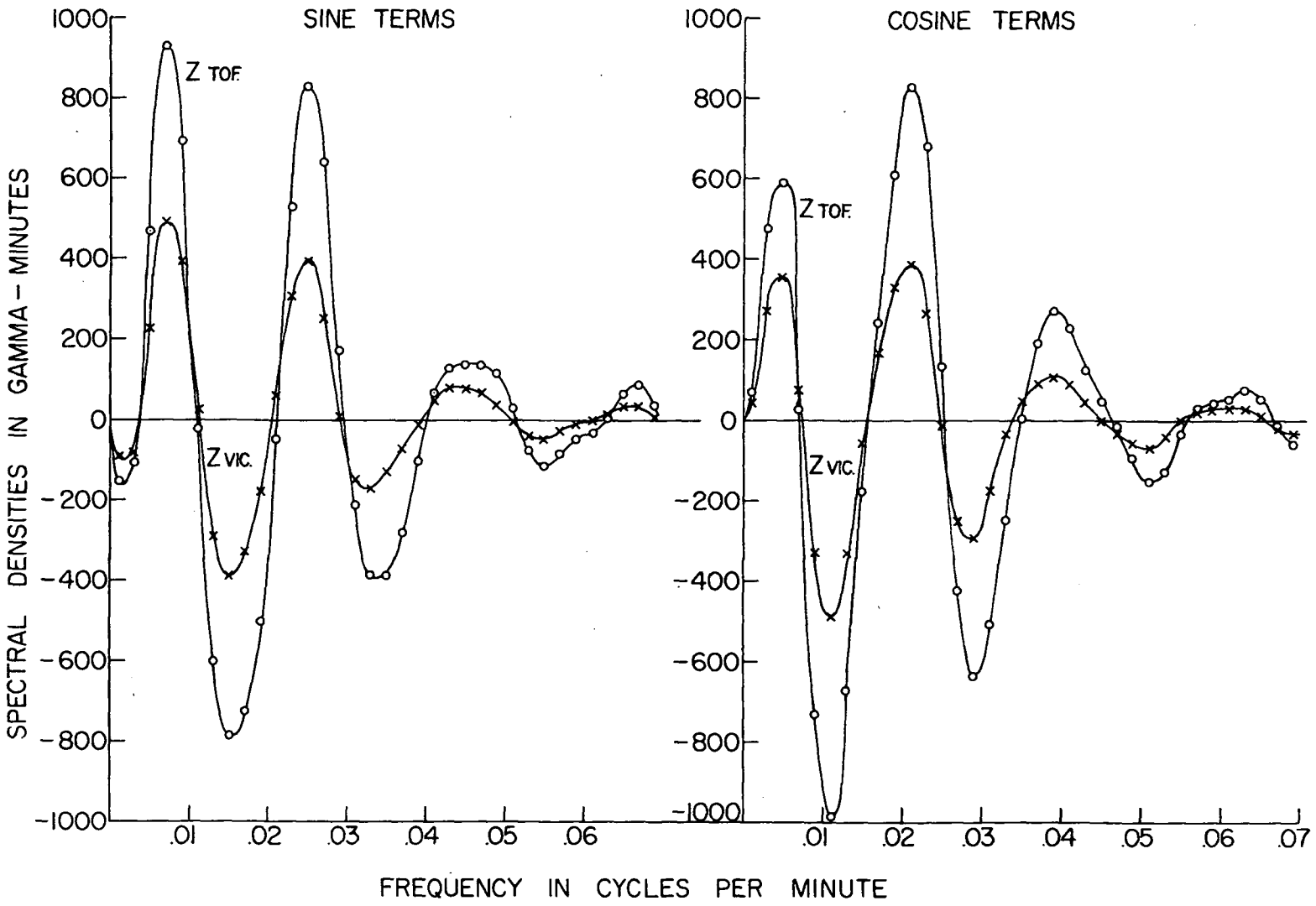

Figure 6 A Comparison of the Sine and Cosine Spectral Densities of the Vertical Component of the Disturbance Recorded at Tofino and Victoria on January 10, 1964

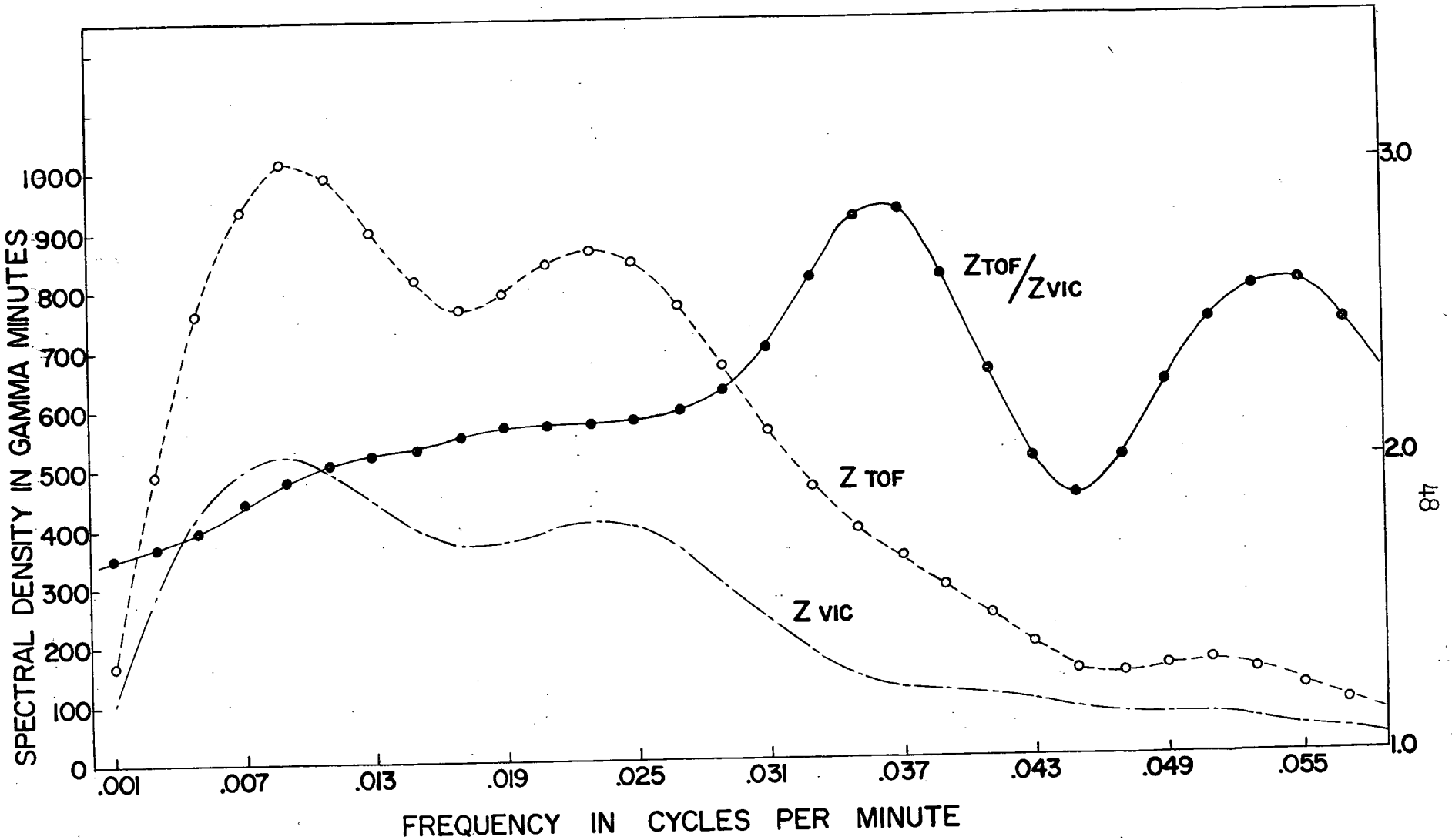

Figure 7. A Comparison of the Amplitude Spectral Densities of the Vertical Component of the Disturbance Recorded at Tofino and Victoria on January 10, 1964

A Directional Dependence of the Anomaly

Nine bay type disturbances were recorded and digitized, covering the period Jan. 10th to July 3rd, 1964. A Fourier Analysis was carried out for each of the three components Z, H, D at all the stations operating at the time of each disturbance. One representative disturbance for each of the five stations was then chosen in order to look for a possible correlation between the vertical and horizontal variations. A plot of the Z, H and D sine and cosine spectral densities for the five stations shows a correlation mostly between the Z and D components, becoming most pronounced at Tofino over the frequency range from one to two cycles per hour (Figs. 8 to 12).

A confirmation of this result was obtained in the form of a polar diagram (Fig. 13). Points representing magnetic variations with frequencies between one and two cycles per hour were derived from the spectral densities of six magnetic disturbances recorded at Tofino. They show a tendency for the field to change upward when it changes to the west and downward when it changes to the east. When the direction of the horizontal change is north or south, very little vertical variation occurs. Although there are only a limited number of points, a correlation in approximately an east-west direction is indicated. The change vectors represented on the polar diagram are scattered about a plane inclined upward towards the west at an angle of about 30° to the horizontal, corresponding to an induction coefficient C = Z/S of 0.5. Points representing field changes with frequencies outside the

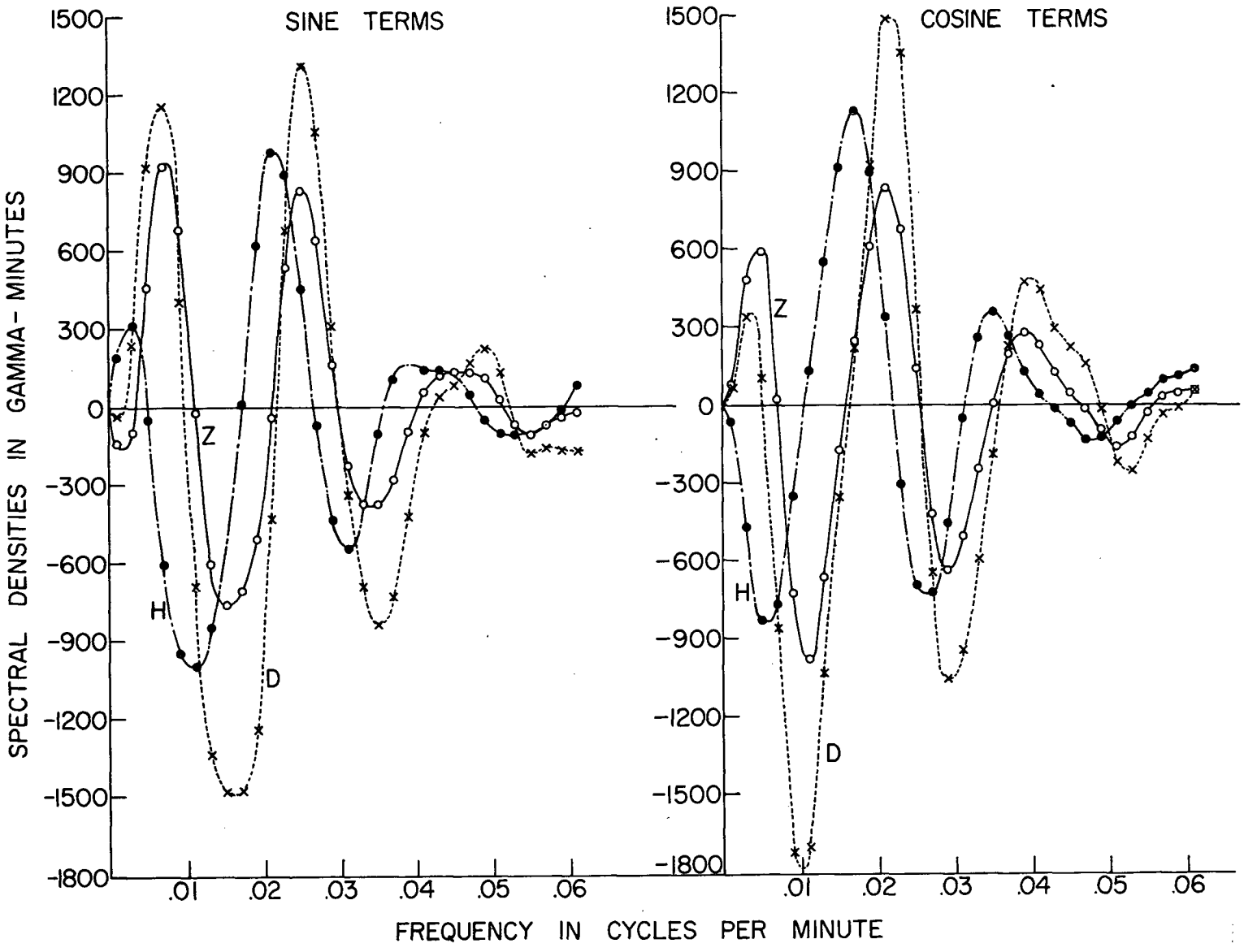

Figure 8 Sine and Cosine Spectral Densities of the D, H and Z components for Magnetic Disturbance Recorded at Tofino on January 10, 1964

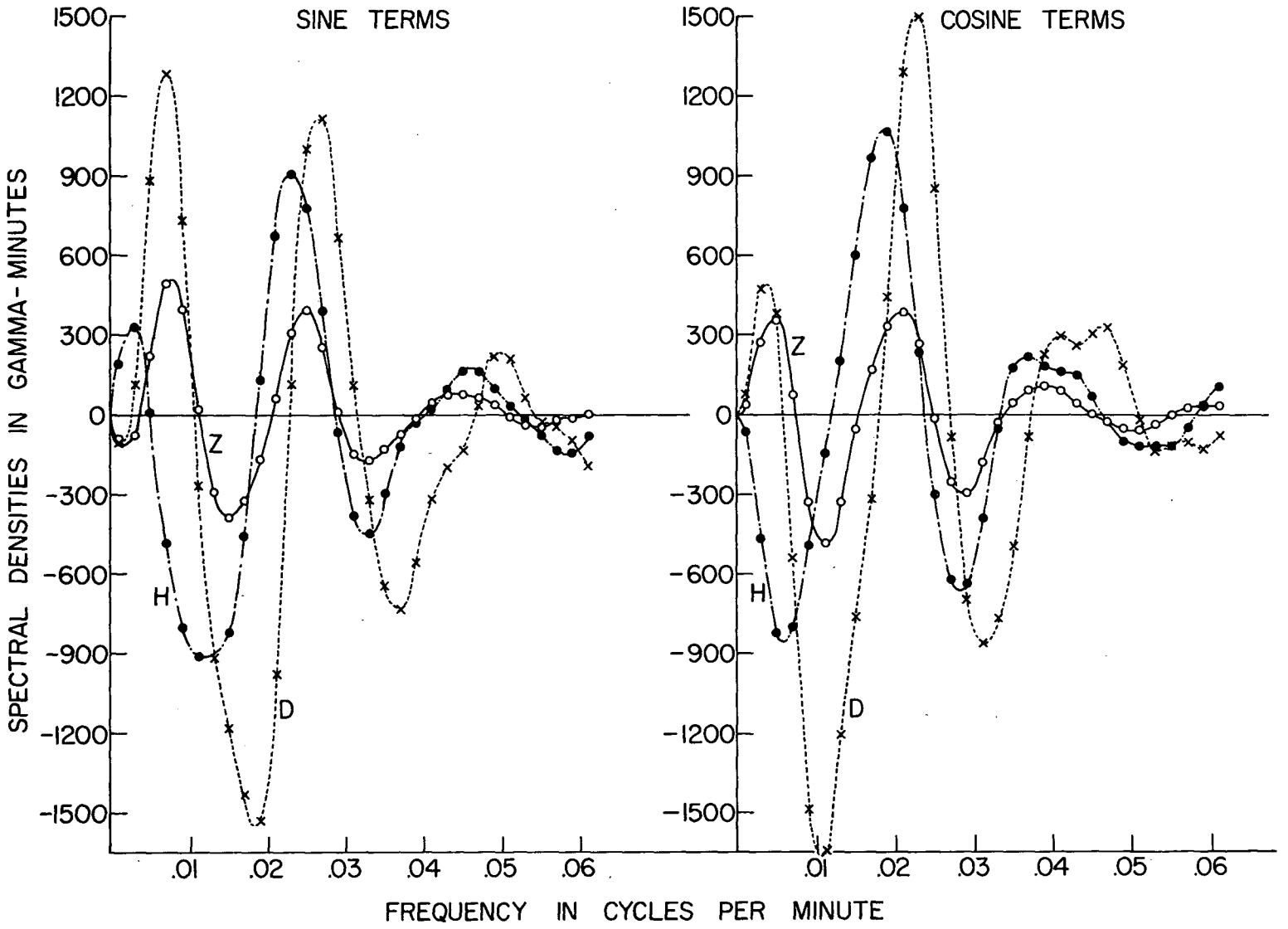

Figure 9 Sine and Cosine Spectral Densities of the D, H and Z components for Magnetic Disturbance Recorded at Victoria on January 10, 1964

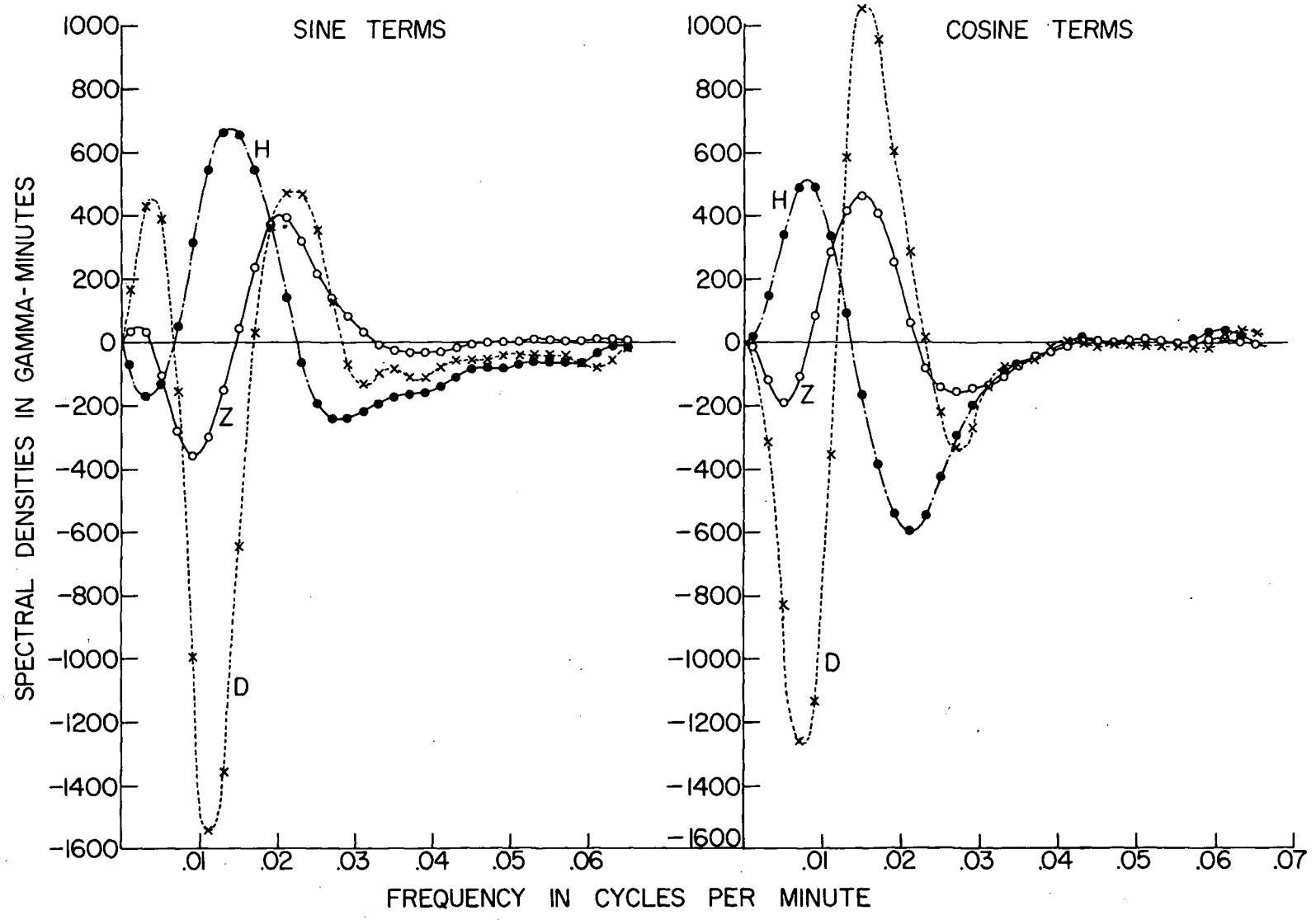

Figure 10 Sine and Cosine Spectral Densities of the D, H and Z Components for Magnetic Disturbance Recorded at Franklin River on July 3, 1964

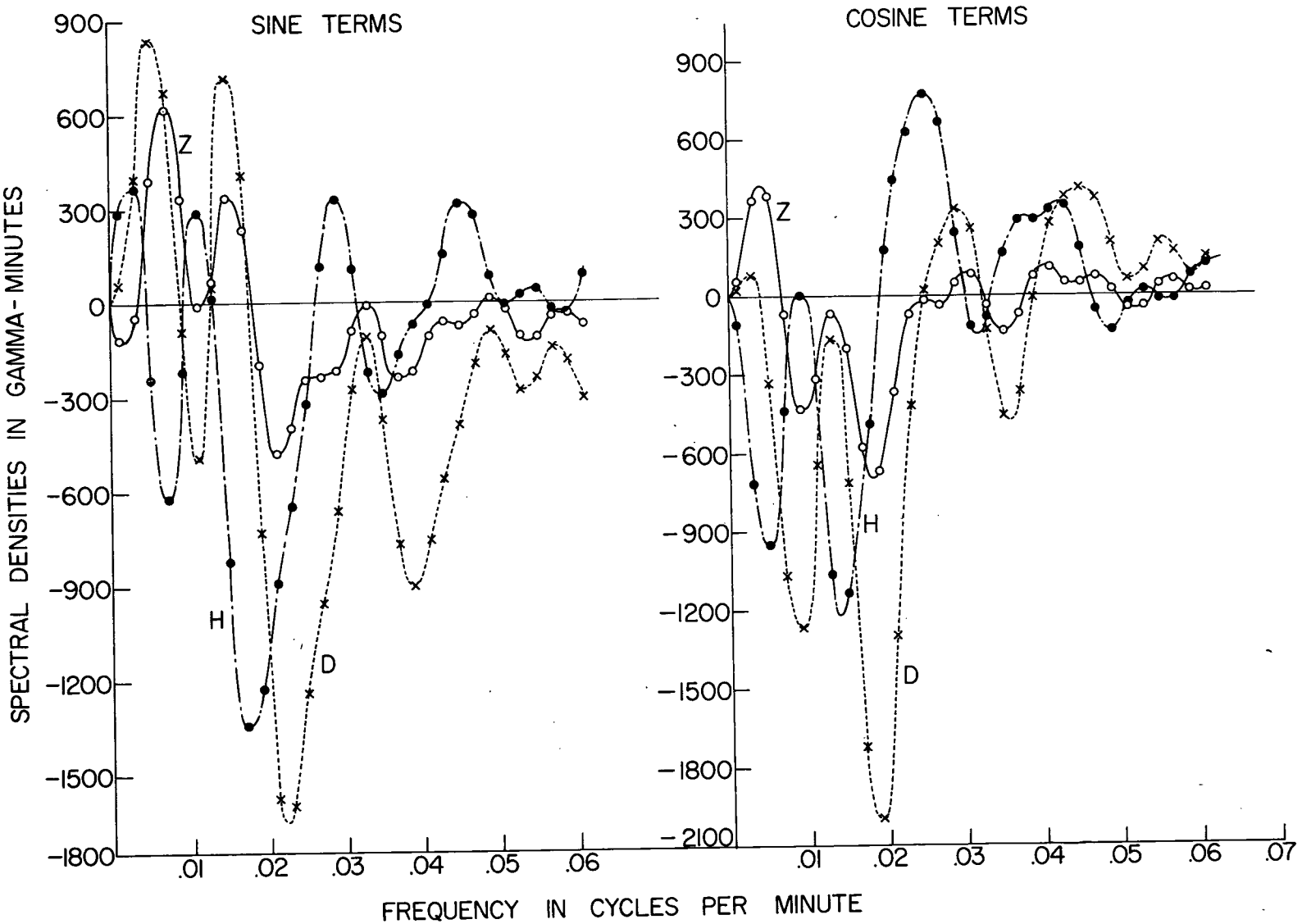

Figure 11 Sine and Cosine Spectral Densities of the D, H and Z components for Magnetic Disturbance Recorded at Westham Island on March 5, 1964

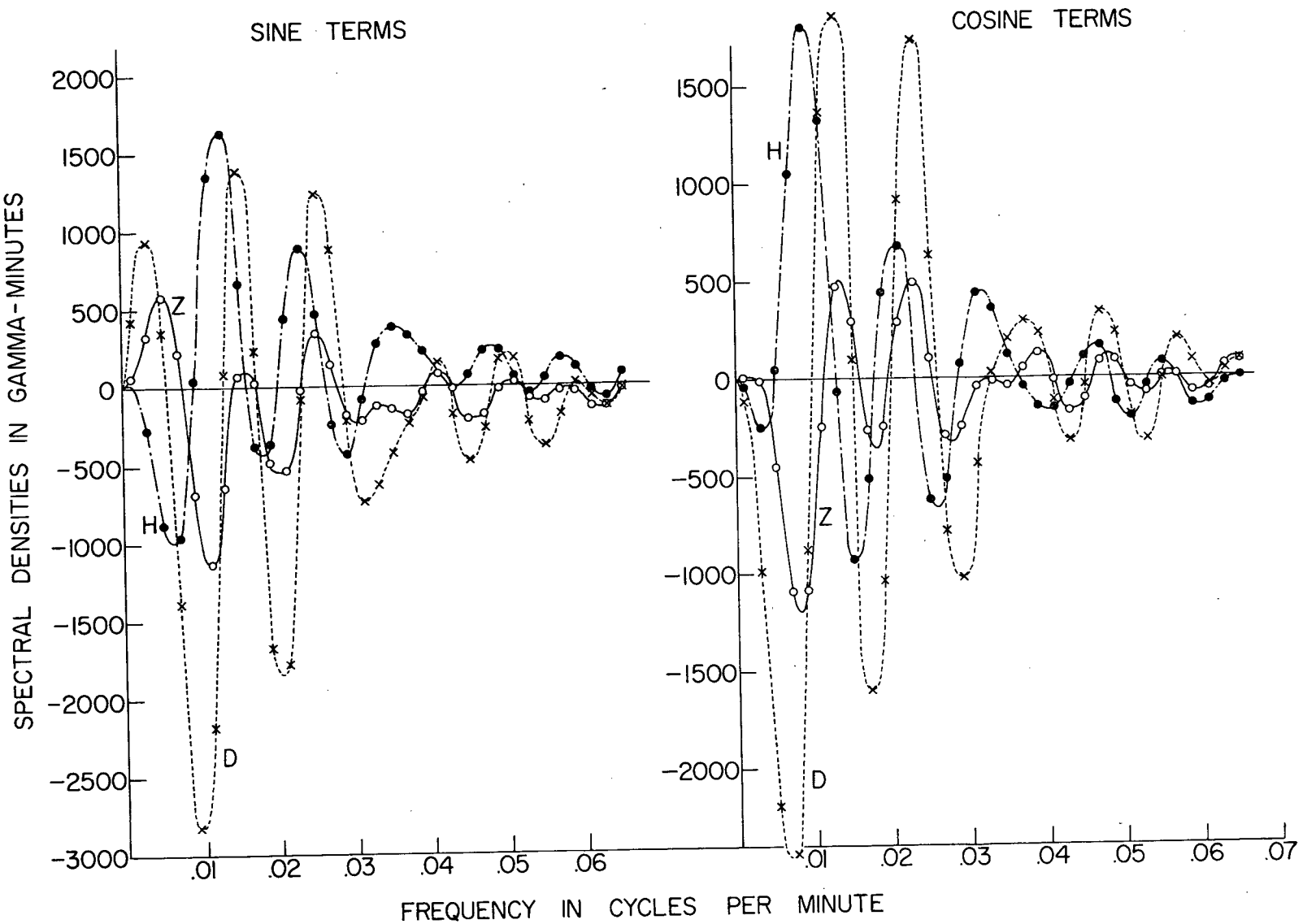

Figure 12 Sine and Cosine Spectral Densities of the D, H, and Z Components for Magnetic Disturbance Recorded at Abbotsford on June 11, 1964

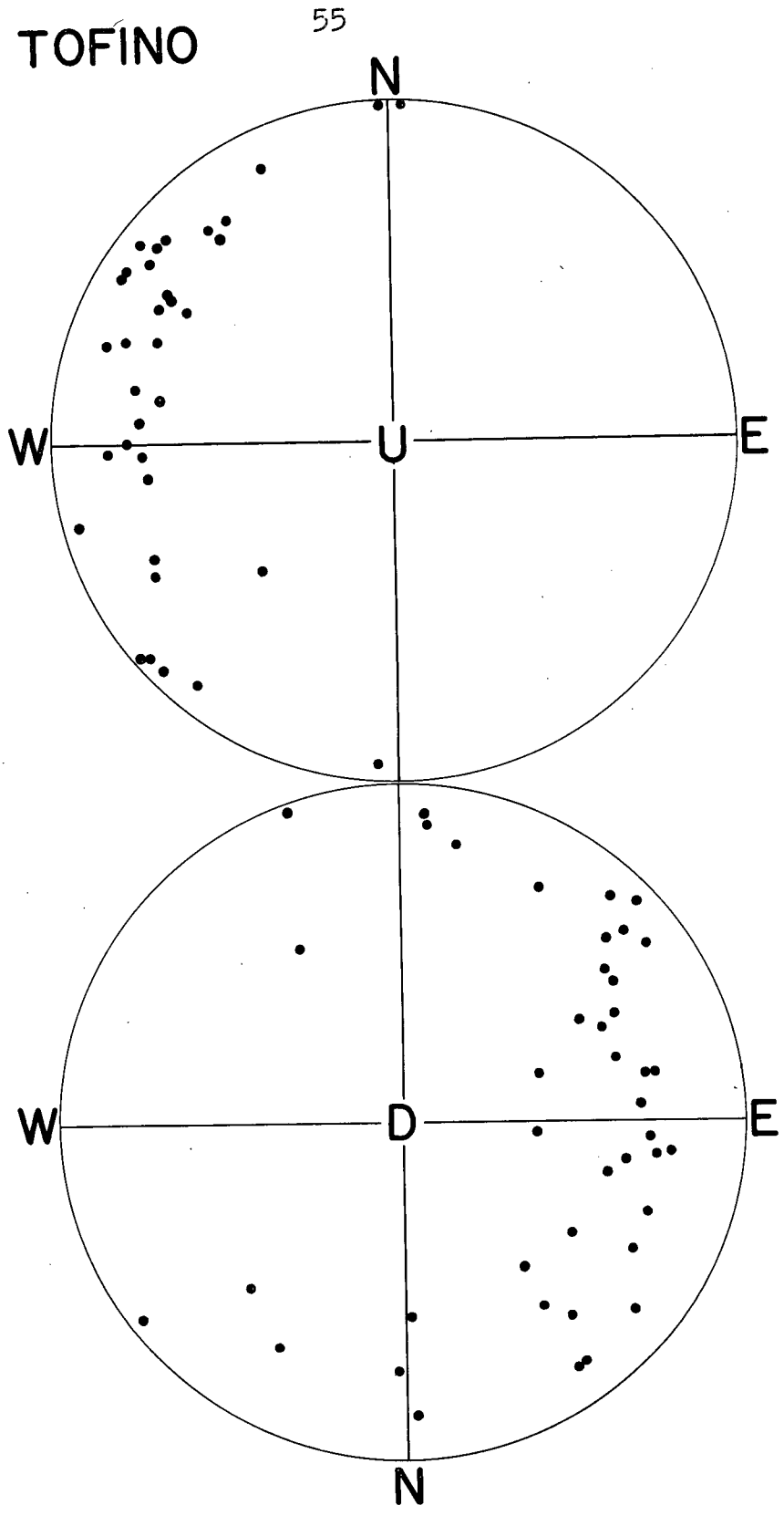

Figure 13 Polar Diagram for Tofino at 30 minute to 60 minute Periods

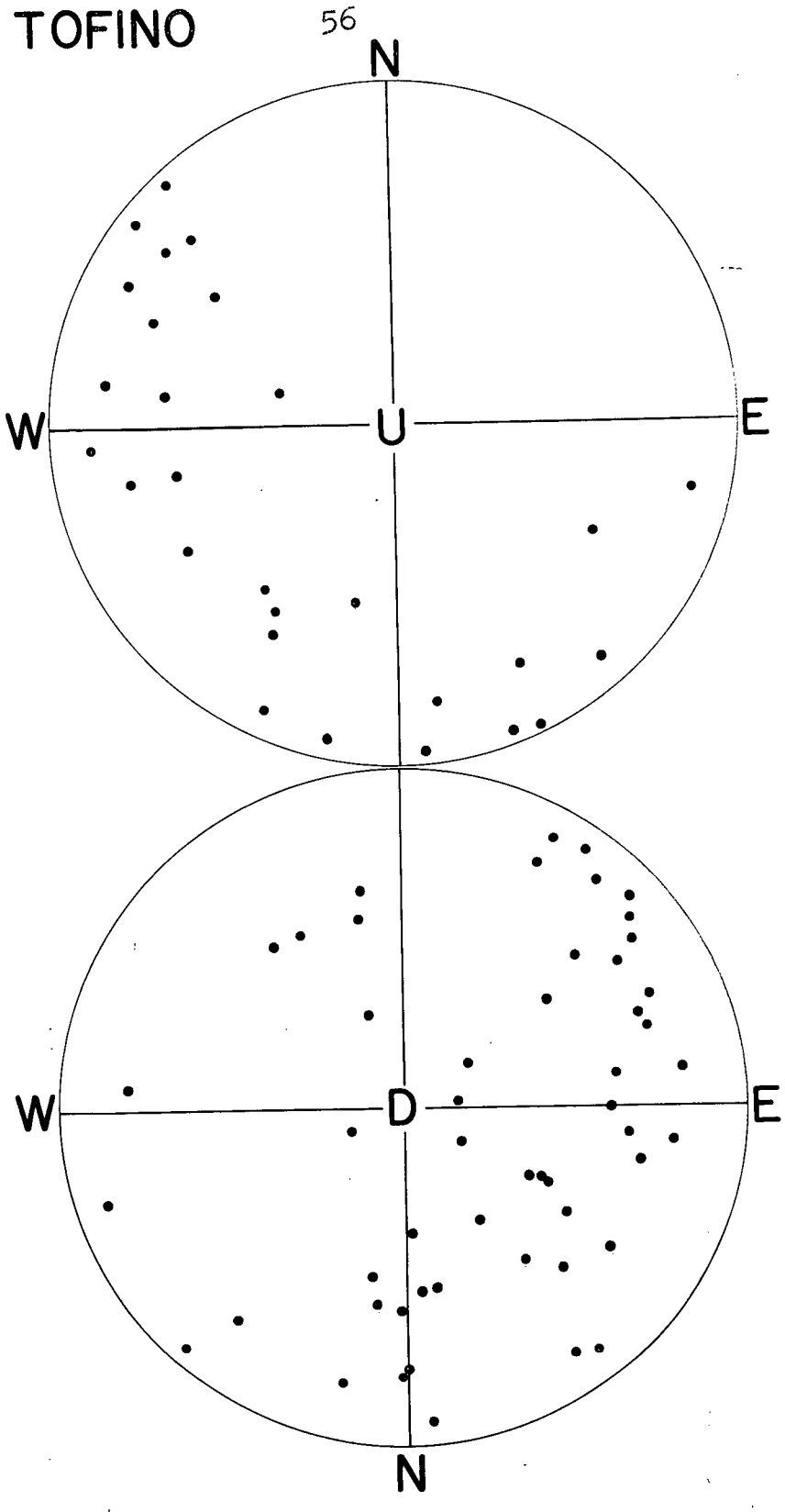

Figure 14 Polar Diagram for Tofino at 20 minute to 25 minute Periods

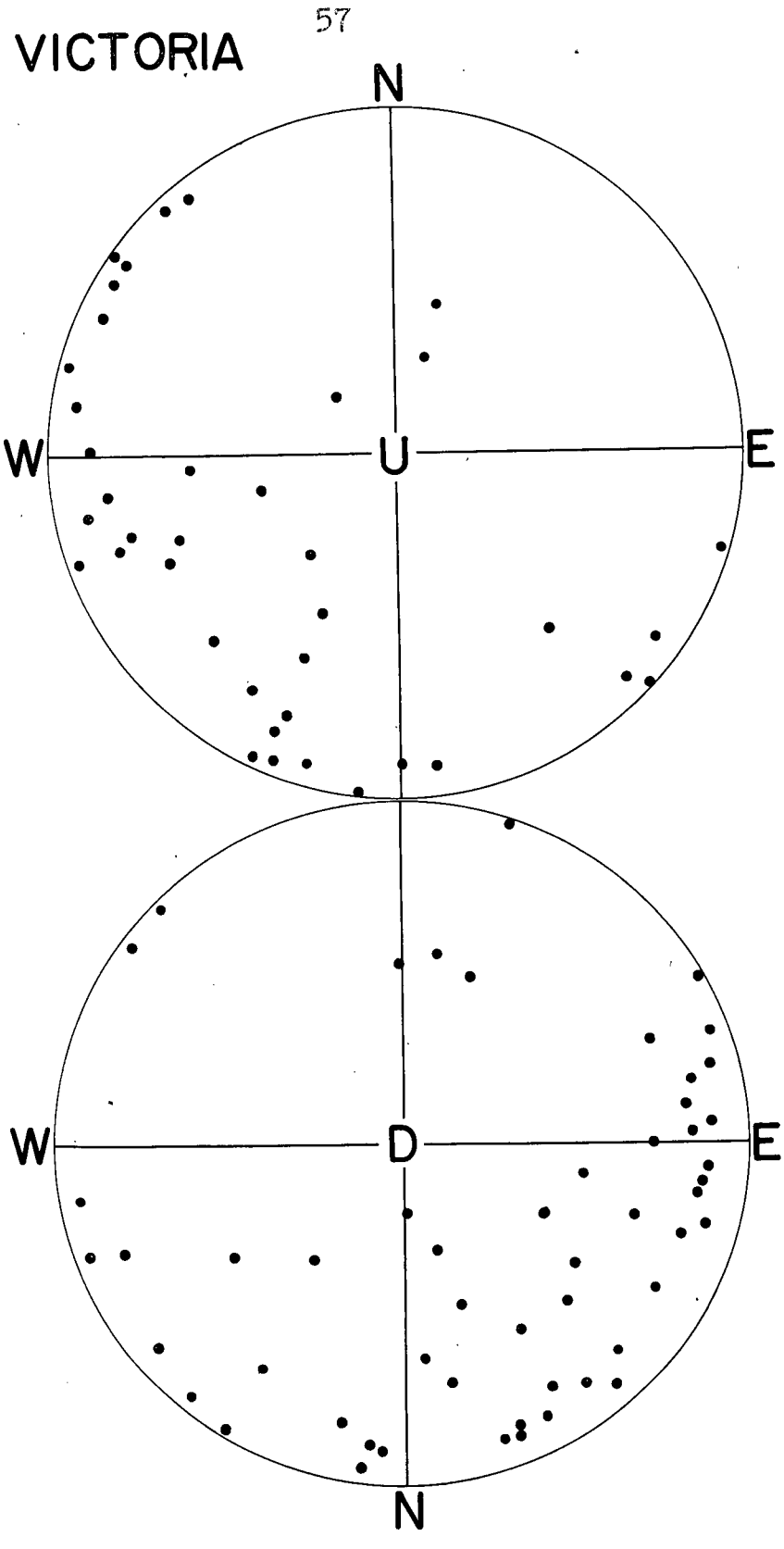

Figure 15 Polar Diagram for Victoria at 30 minute to 60 minute Periods

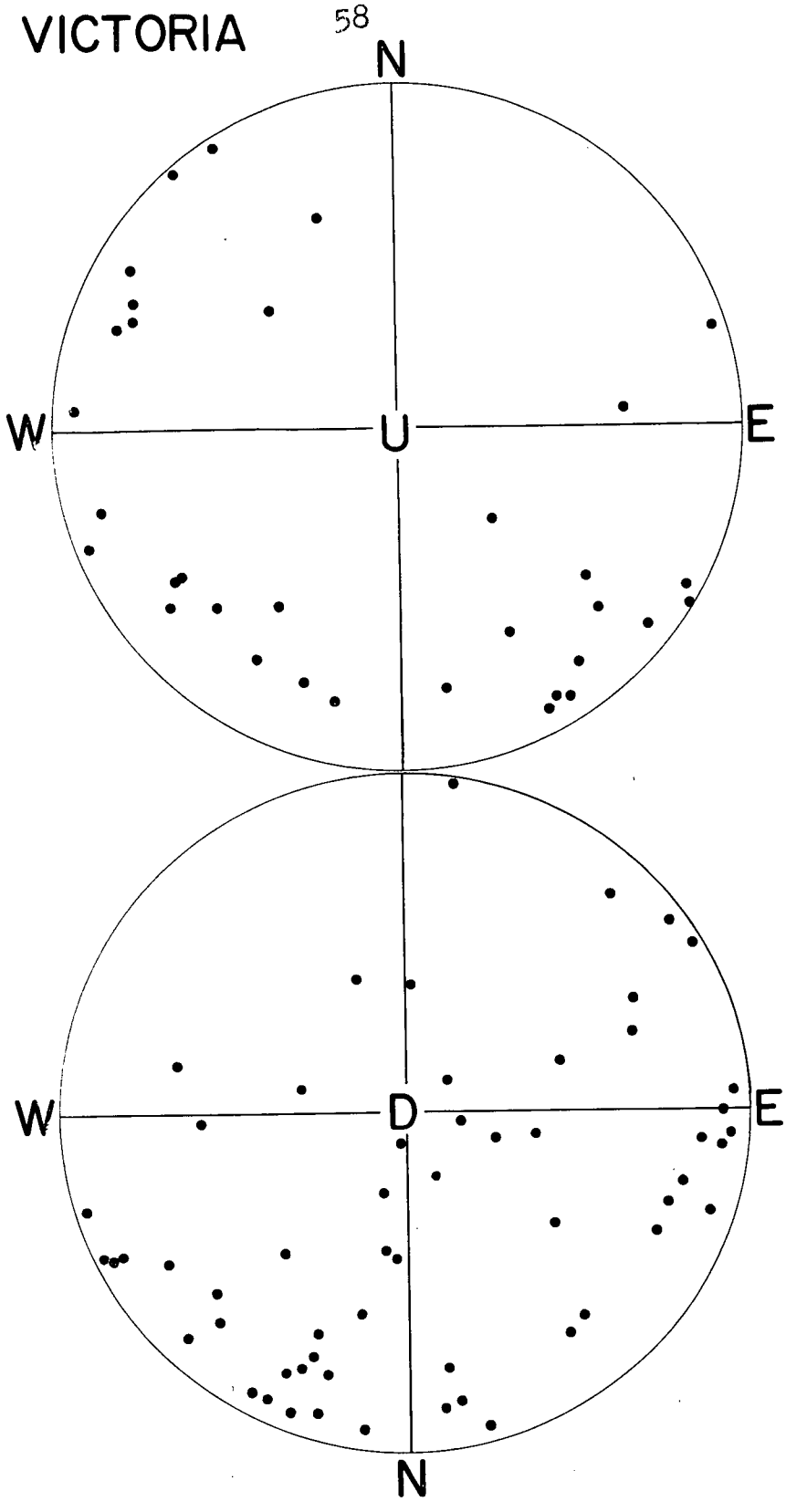

Figure 16 Polar Diagram for Victoria at 20 minute to 25 minute Periods

range one to two cycles per hour, not included on this polar diagram, deviated considerably from this pattern, indicating that the coastal anomaly is most clearly defined in this frequency range.

The Z, H and D sine and cosine spectral densities for Tofino at a frequency of about three cycles per hour show that the Z component is not correlated with the D or H component alone but probably with a combination of both. A polar diagram plotted for Tofino at the higher frequency shows a correlation in a north-east, south-west direction approximately perpendicular to the Vancouver Island coastline, but the scatter in the points is greater than at the lower frequencies making it difficult to define a preferred plane (Fig. 14).

Polar diagrams plotted for Victoria were based essentially on the same magnetic disturbances that were utilized in the Tofino diagrams. The correlation at frequencies of one to two cycles per hour at Victoria appears to be more north-east, south-west rather than east-west as at Tofino with a great deal more scatter than on the corresponding Tofino diagram (Fig. 15). At a frequency of three cycles per hour the correlation is not clear (Fig. 16).

B Spatial Dependence of the Anomaly

The stations occupied along the east west profile provided a means of measuring the coastal anomaly at distances of 50, 120, 240, and 300km. east of the one hundred fathom line off the west coast of Vancouver Island. The spatial dependence is best studied

by analyzing magnetic disturbances recorded simultaneously at all stations on the profile. However, each magnetic disturbance was recorded only at two or three of the stations, because of frequent instrument failures, mainly in the drive unit, and local artificial disturbances at the Tofino station. In addition, the two stations at the eastern end of the profile were at no time occupied simultaneously. Thus, comparisons of the vertical and horizontal variations between two stations on the profile could sometimes be made only indirectly with reference to the Victoria station.

1. Variations with a Period of Forty Five Minutes

The vertical variations, Z, at this period are apparently correlated with the component of the horizontal disturbance in an east-west direction, S. A study of the change of Z and S with distance along the profile illustrates the spatial dependence of the anomaly. The amplitude spectral densities $C_z(\omega)$ represent the vertical variation, Z, at each frequency ω and the east-west horizontal variation S is defined using the sine and cosine spectral densities $A_H(\omega)$, $B_H(\omega)$, $A_D(\omega)$ and $B_D(\omega)$ of the H and D components.

Vertical Component

Amplitude spectral densities, $C(\omega)$, at frequencies of .021, .023 and .025 cycles per minute represent variations with a period of approximately forty five minutes. A comparison of $C_z(\omega)$ along the profile at these frequencies, for the same magnetic disturbance, furnishes a fairly consistent pattern (Table 6).

For the six magnetic features studied, the values of Z decrease from Tofino to the Westham Island and Abbotsford stations, the value at Tofino being as much as one hundred percent larger than at Westham Island. A mean value of Z was calculated for each station by normalizing the vertical component of each disturbance by the corresponding vertical component at Abbotsford (Table 2). (In some cases this was calculated indirectly by comparison with Victoria values.) This mean value of Z decreases steeply from Tofino to Franklin River and then less steeply towards the representative inland stations of Westham Island and Abbotsford (Fig. 19), the latter stations being equivalent if a confidence level of twenty percent is accepted. An important point is that the Tofino anomaly diminishes to less than half its value over the 70 kilometer distance from Tofino to Franklin River. On the average Victoria values do not differ significantly from Abbotsford values.

Horizontal Components

The component of the horizontal variation in an east-west direction, S, at a period of forty five minutes, in general decreases coastward with the exception that in some cases Franklin River has a slightly smaller value than Tofino (Table 6). The value of S at Tofino, however, is consistently about five to ten percent smaller than at Westham Island. With reference to Abbotsford a mean value of S was calculated for each station with a probable error of three percent (Table 2). The decrease of ten percent in the mean value of S from Abbotsford to Tofino is

consistent with the expected decrease with distance from the Auroral Zone. If the source of geomagnetic bays is assumed to be a linear current approximately 2000km. from the profile, the horizontal component falls off in inverse ratio to the square of the distance from the source (Van'yan and Kharin(52))

i.e. $$S = \frac{K}{r^2}$$

and hence $$dS = -\frac{2K}{r^3}\,dr = -S\,\frac{2dr}{r}$$

Tofino is about 100 kilometers further from the Auroral Zone than Abbotsford, so that

$$\frac{dS}{S} = -\frac{2dr}{r} = \frac{-2(100)}{2000} = -0.1$$

Thus, a decrease of ten percent in the value of S is expected, independent of an internal anomaly. In the light of these considerations, no anomaly is apparent in the horizontal component.

The Induction Coefficient Z/S

The correlation exhibited by the Tofino polar diagram for frequencies between one and two cycles per hour justifies the calculation of an induction coefficient C = Z/S at a period of forty-five minutes. The mean of the Z/S ratios given in (Table 6) is 0.5 ± .03 which is consistent with the 30° tilt of the preferred plane on the polar diagram and comparable to the values obtained by Parkinson(25) in Australia.

2. Variations with a Period of Twenty Minutes

The scatter of the Tofino polar diagram at a frequency of

three cycles per hour is too great to justify correlating the vertical variations with a horizontal disturbance vector in a particular direction.

Vertical Component

Amplitude spectral densities $C(\omega)$ at frequencies of .047, .049, .051, and .053 cycles per minute were used to represent variations with a period of approximately twenty minutes. The vertical component at Tofino is typically larger than at Franklin River but, instead of there being a smooth trend to smaller values further inland, values at Victoria, Westham Island and Abbotsford are in general larger than at Franklin River, but usually not so large as at Tofino (Table 5). As at the lower frequency a mean value of Z, based on eight magnetic features, was calculated for each station relative to corresponding Abbotsford values (Table 2). The plot of Z as a function of distance from the coast shows the Tofino anomaly and also suggests a vertical anomaly in the region of Westham Island (Fig. 19). The larger probable errors at this frequency imply that the suggested trends are not as consistently reproducible as at the lower frequencies. Nevertheless, the enhancement of Westham Island over Abbotsford which is absent at the lower frequencies is statistically significant and most likely does reflect a relatively shallow conductivity inhomogeneity.

Horizontal Component

The total horizontal variation H_t is, in general, larger inland, the amplitudes at Westham Island being about twenty percent

larger than at Tofino and the amplitude at Franklin River usually from ten to twenty percent larger (Table 5). Here again, the horizontal variations are expected to diminish with increasing distance from the Auroral Zone. Hence, we conclude as before, that no appreciable internal anomaly shows up in the horizontal component from Tofino to Abbotsford.

C Frequency Dependence of the Anomaly

The vertical amplitude spectral densities, $C_z(\omega)$, at Tofino and Franklin River were compared with the corresponding values at Victoria (Table 3). The values of $Z_{TOF.}/Z_{VIC.}$ derived from six magnetic disturbances showed a statistically significant deviation from a postulated value $Z_{TOF.}/Z_{VIC.} = 1$ over the entire range of periods from twenty minutes to three hours. The values of $Z_{FRA.}/Z_{VIC.}$ derived from five magnetic disturbances did not deviate significantly from a ratio of unity over the same frequency range, and a comparison between Victoria and Abbotsford at these frequencies based on six magnetic features showed no significant difference.

The mean values of $Z_{TOF.}/Z_{VIC.}$ and $Z_{FRA.}/Z_{VIC.}$ were plotted as a function of period and the points fitted with a smooth curve (Fig. 17). The results indicate that the anomaly reaches a maximum at a period of thirty minutes to one hour, a period at which the effective overall conductivity contrast is apparently greatest.

D Daily Geomagnetic Variations

A Fourier analysis of sixty hours of simultaneous magnetic

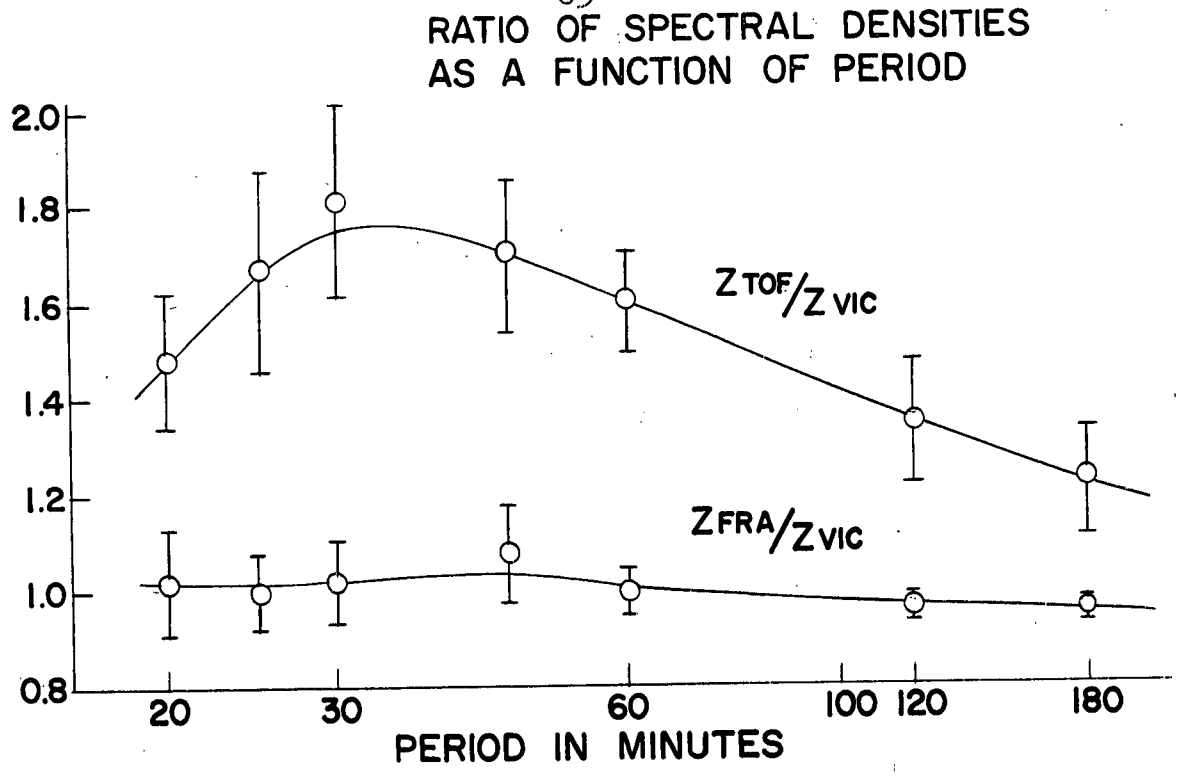

Figure 17. Frequency Dependence of the Tofino Anomaly

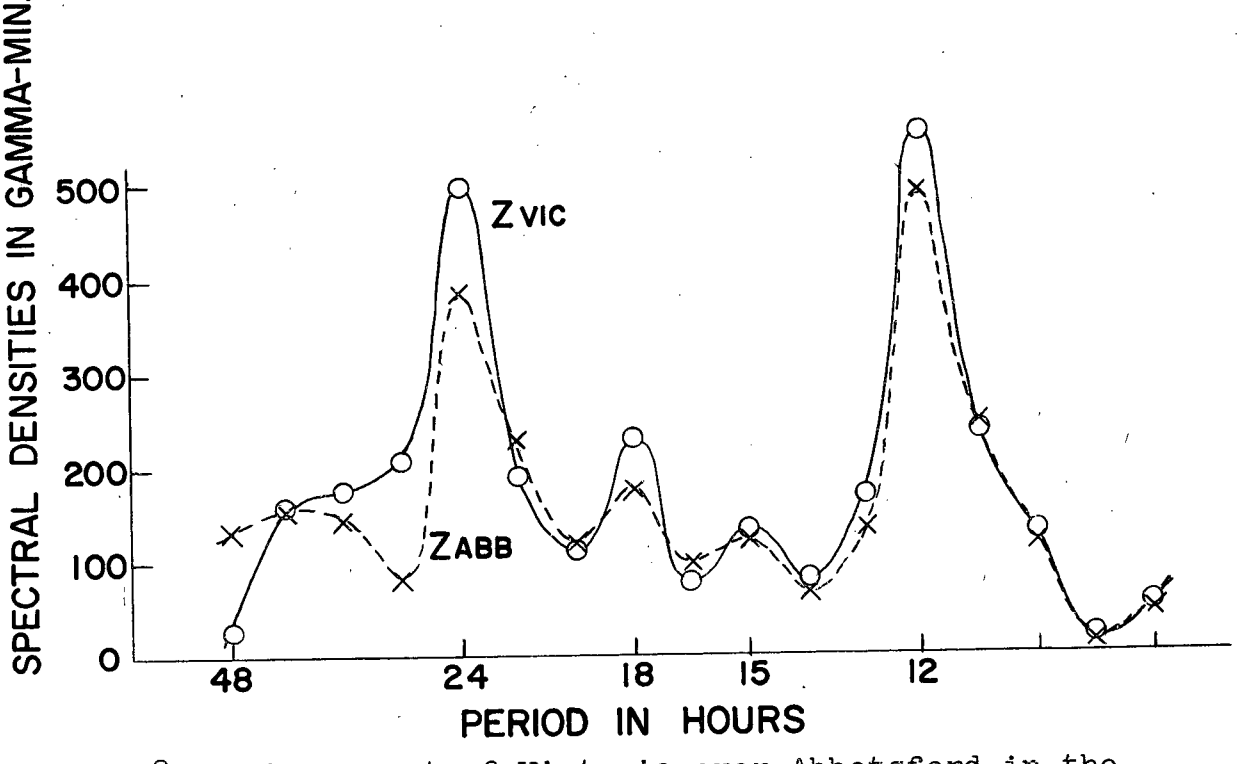

Figure 18. Enhancement of Victoria over Abbotsford in the Vertical Components at the Diurnal and Semi-Diurnal Periods

records at Tofino, Franklin River, Victoria, and Abbotsford yielded well defined peaks at periods of twelve and twenty-four hours, allowing a comparison of the diurnal and semi diurnal geomagnetic variations at these four stations. Additional analyses of simultaneous records were not possible because of local disturbances on the Tofino records, so that these results must be considered as preliminary. There are no convincing trends in the horizontal components of the semi diurnal variations, but there is a six percent increase in the diurnal horizontal component from Abbotsford to the coast (Table 4). However, the vertical variations for both the diurnal and semi diurnal components decrease eastward along the profile Tofino, Franklin River, Abbotsford, the amplitude of the Vancouver Island stations, including Victoria, being twenty to thirty percent larger than at Abbotsford on the mainland.

The marked difference in the vertical daily variations between Abbotsford and the more western stations indicated in the above preliminary analysis had been mentioned in an earlier study by Hyndman[16]. Consequently, a more thorough analysis based on one hundred and twenty-six consecutive hours of simultaneous magnetic records was carried out in order to compare the vertical variations at the Victoria and Abbotsford stations. The results show a twenty five percent enhancement of Victoria over Abbotsford in the diurnal vertical variations, diminishing to a ten percent enhancement in the semi diurnal vertical variations (Fig. 18). Victoria does not differ appreciably from Abbotsford at higher frequencies.

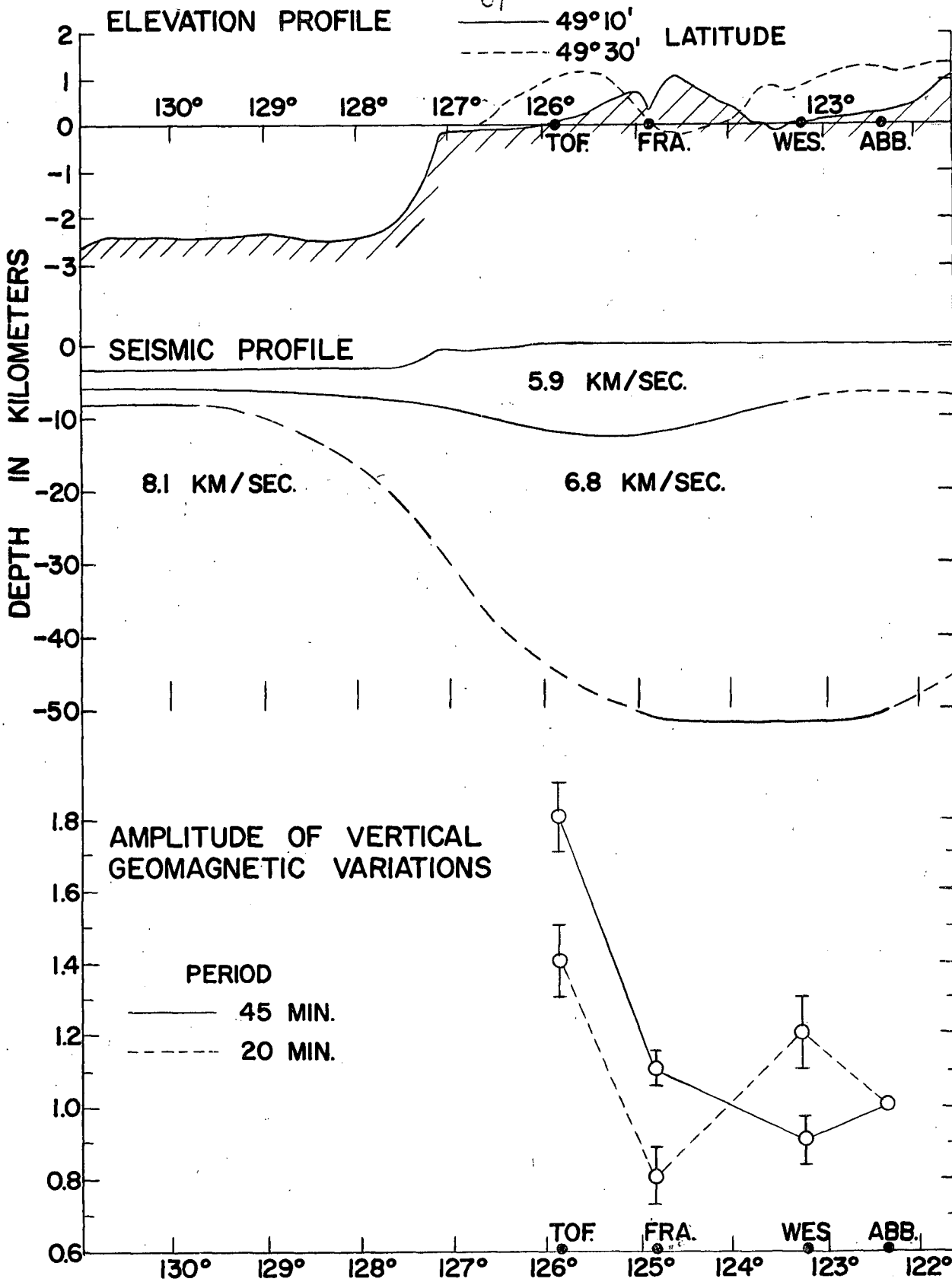

Figure 19. Amplitude of Vertical Variations along the East-West Profile Normalized with Abbotsford Values; Compared with an Elevation Profile and a Crustal Structure Profile (adapted from W.R.H. White and J.C. Savage)

E Discussion of Results

The vertical anomaly at Tofino reaches a maximum at a frequency between one and two cycles per hour and is characterized by an induction coefficient of 0.5. The polar diagram plotted for this range of frequencies suggests a two dimensional conductivity discontinuity running approximately in a north-south direction. Although the diagram at a higher frequency of three cycles per hour seems to indicate a shift in the directional dependence (more perpendicular to the coastline), such a shift cannot be considered significant because of the limited number of points and the scatter on the diagrams. It is clear, however, that at the maximum response frequency the directional dependence is consistent with that expected at the edge of an oceanic current sheet and/or above a two dimensional conductivity step in the upper mantle running approximately parallel to the continental shelfline. Since the anomaly diminishes to an almost negligible value at a distance of 100 kilometers from the coastline (Fig. 19) it is not expected to be caused by a conductivity step deeper than 100 kilometers beneath the surface. Furthermore, unless the upper surface of the step is at a shallow depth, perhaps in the vicinity of the Mohorovičič discontinuity, most of the electric currents will flow in the ocean rather than in the mantle beneath. Until one can accurately measure the electric currents flowing in the deep ocean or the amplitude of geomagnetic variations beneath the oceanic layer, it is difficult to estimate the contribution of subsurface changes in conductivity at the coastline.

The twenty-five percent increase in the vertical diurnal variations from the mainland to Vancouver Island must be independent of surface layers and most likely does reflect some kind of lateral subsurface change in conductivity deep in the upper mantle which may be associated with a systematic difference in the nature of the upper mantle beneath oceans and continents.

The possible vertical anomaly at three cycles per hour at Westham Island may be due to a relatively shallow conductivity inhomogeneity, since it is absent at a lower frequency of one to two cycles per hour. The limited spatial extent of the coastal anomaly rules out mutual induction between the Pacific Ocean and the sea water in Georgia Strait, and the total conductivity of the sea water is not large enough to sustain electric currents for longer than a few seconds. However, the Georgia Strait depression at the south end of the largely submerged coastal trough between Vancouver Island and the mainland is underlain to a depth of five kilometers by clastic sediments of late Mesozoic and early Cenozoic age (White and Savage[58]). Consequently, it is at least plausible to suppose that the overall conductivity of the depression relative to the mainland rocks is large enough to cause a small vertical anomaly. At the same time, a deeper subcrustal source is not ruled out.

VI CONCLUSIONS

With reference to Fig. 19 which shows the magnitude and extent of the vertical anomaly, an elevation profile for the region, and a crustal structure profile based on seismic and gravity data (White and Savage[58]), it is believed that:

(a) The major portion of the coastal anomaly at one to two cycles per hour is caused by electric currents flowing in the ocean beyond the continental shelfline, unless there is a lateral conductivity contrast at a depth of 100km or less which is large enough to compete with the contrast between ocean and continent.

(b) The extent of the diurnal "anomaly" is consistent with a conductivity discontinuity deep in the upper mantle.

(c) The possible inland anomaly at a higher frequency of three cycles per hour is so heavily dependent on shallow structure that no consistent trends compatible with the large scale crustal model can be postulated.

TABLES

STATION	INSTRUMENT	GEOGRAPHIC LONGITUDE	LATITUDE	APPROX. ELEVATION (FT)	DURATION OF OBSERVATIONS
TOFINO	ASKANIA	125°47'W	49°5'N	40	Dec 16/63 to July 10/64
FRANKLIN RIVER	ASKANIA	124°48'W	49°6'N	100	May 16/64 to July 10/64
VICTORIA	ASKANIA	123°25'W	48°31'N	600	Sept 1/63 to May 12/64
VICTORIA	RUSKA	123°25'W	48°31'N	600	Continuous
WESTHAM ISLAND	ASKANIA	123°11'W	49°6'N	10	Nov 1/63 to June 5/64
ABBOTSFORD	ASKANIA	122°21'W	49°1'N	200	June 5/64 to July 12/64

Table 1 Location and Details of the Variograph Stations

FREQUENCY RANGE	.021 C.P.M. to .025 C.P.M. TOF	FRA	WES	ABB		.047 C.P.M. to .053 C.P.M. TOF	FRA	WES	ABB
Z COMPONENT	1.8±0.1	1.1±.04	0.9±.07	1.0	Z COMPONENT	1.4±0.1	0.80±.08	1.2±0.1	1.0
S COMPONENT	0.9±.03	0.9±.02	1.0±.04	1.0	H_t COMPONENT	0.9±.05	1.0±.03	1.1±.09	1.0
	VIC					VIC			
	1.1±0.09					1.0±0.1			

Table 2 Mean Values of Vertical and Horizontal Changes Relative to Abbotsford Values (Based on Nine Magnetic Disturbances)

FREQUENCY IN CYCLES PER MIN	JAN. 10, 1964		MARCH 5, 1964		MAY 24, 1964			JUNE 19, 1964	
	TOF	VIC	TOF	VIC	TOF	FRA	VIC	FRA	VIC
.005	760	420	550	340	2790	2740	2890	3610	3840
.009	1010	520	680	430	2540	2150	2000	2420	2650
.017	760	370	1050	540	810	530	560	1400	1450
.023	860	410	850	410	580	450	450	720	750
.033	460	170	110	40	370	340	340	140	60
.041	240	100	360	170	130	80	90	420	470
.049	150	70	70	50	170	170	170	180	240

	MAY 25, 1964			MAY 27, 1964			JUNE 21, 1964		
	TOF	FRA	VIC	TOF	FRA	VIC	TOF	FRA	VIC
.005	4160	4100	4520	1940	1720	1580	920	970	1060
.009	2880	2780	2940	930	610	560	450	550	660
.017	400	350	400	690	500	400	230	170	170
.023	460	360	460	250	170	100	220	170	170
.033	360	200	270	160	130	90	120	90	100
.041	220	260	300	140	80	60	130	130	160
.049	210	160	200	80	70	40	40	30	40

Table 3 Comparison of Vertical Component Spectral Densities (in Gamma-minutes) at Tofino, Franklin River and Victoria as a Function of Frequency.

VERTICAL COMPONENT	TOF	FRA	VIC	ABB
DIURNAL	525	490	508	406
SEMI DIURNAL	333	285	290	278
TOTAL HORIZONTAL COMPONENT				
DIURNAL	876	854	825	830
SEMI DIURNAL	670	679	648	687

Table 4 Comparison of Spectral Densities for the Daily Variations (Based on 60 hrs. of Continuous Records from 1500 U.T. June 19/64 to 9300 U.T. June 22/64)

.047 CYCLES PER MINUTE

DATE OF FEATURE	Z COMPONENT TOF	FRA	WES	ABB	VIC*	H_t COMPONENT TOF	FRA	WES	ABB	VIC*	Z/H_t RATIO TOF	FRA	WES	ABB	VIC*
JAN. 10	140				70	270				360	0.5				0.2
MARCH 5	130		80		40	450		510		440	0.3		0.2		0.1
MAY 24	190	150	180		180	90	100	130		120	2.0	1.4	1.4		1.5
APRIL 29			40		10			190		190			0.2		0.1
MAY 25	270	240			310	300	290			240	0.9	0.8			1.3
MAY 27	90	50			60	290	180			290	0.3	0.3			0.2
JUNE 21	70	50		70	50	150	170		180	170	0.4	0.3		0.4	0.3
JUNE 10		150		160	180		320		370	290		0.5		0.4	0.6
JULY 3		10		30			100		80			0.1		0.4	

.049 CYCLES PER MINUTE

JAN 10	150				70	280				310	0.5				0.2
MARCH 5	70		20		50	230		270		220	0.3		0.1		0.2
MAY 24	170	170	210		170	90	100	120		120	1.9	1.6	1.8		1.5
APRIL 29			10		20			150		130			0.1		0.1
MAY 25	210	160			200	200	250			240	1.1	0.6			0.9
MAY 27	80	70			40	140	110			120	0.6	0.6			0.3
JUNE 21	40	30		60	40	140	150		190	160	0.3	0.2		0.3	0.2
JUNE 10		180		170	240		360		420	350		0.5		0.4	0.7
JULY 3		10		30			90		80			0.1		0.3	

Table 5 Comparison along the Profile of the Spectral Densities (in Gamma-minutes) Representing the Vertical Change Z and the Total Horizontal Change H_t together with the Ratio Z/H_t (Victoria Not Included in the Profile)

.051 CYCLES PER MINUTE

DATE OF FEATURE	Z COMPONENT TOF	FRA	WES	ABB	VIC*	H_t COMPONENT TOF	FRA	WES	ABB	VIC*	Z/H_t RATIO TOF	FRA	WES	ABB	VIC*
JAN 10	160				60	290				250	0.5				0.3
MARCH 5	50		60		70	140		180		140	0.4		0.3		0.5
MAY 24	170	150	170		150	60	70	80		90	2.6	2.1	2.1		1.7
APRIL 29			50		50			140		110			0.3		0.4
MAY 25	290	240			250	240	330			340	1.2	0.7			0.7
MAY 27	100	80			70	170	180			170	0.6	0.5			0.4
JUNE 21	30	30		20	40	100	100		130	110	0.3	0.3		0.1	0.4
JUNE 10		160		170	200		370		460	310		0.4		0.4	0.6
JULY 3		10		20			90		80			0.1		0.2	

.053 CYCLES PER MINUTE

JAN 10	140				60	290				200	0.5				0.3
MARCH 5	100		110		70	260		300		260	0.4		0.4		0.3
MAY 24	90	70	100		80	150	150	140		120	0.6	0.5	0.8		0.7
APRIL 29			70		60			140		120			0.5		0.5
MAY 25	370	320			340	290	350			350	1.3	0.9			1.0
MAY 27	70	30			40	210	210			220	0.3	0.2			0.2
JUNE 21	40	40		30	50	70	80		80	60	0.6	0.5		0.4	0.9
JUNE 10		160		200	150		290		370	250		0.5		0.5	0.6
JULY 3		10		10			80		70			0.2		0.1	

Table 5 (continued)

.021 CYCLES PER MINUTE

DATE OF FEATURE	Z COMPONENT TOF	FRA	WES	ABB	VIC*	S COMPONENT TOF	FRA	WES	ABB	VIC*	Z/S RATIO TOF	FRA	WES	ABB	VIC*
JAN 10	840				390	1500				1620	0.6				0.2
MARCH 5	1100		600		560	1970		2060		1890	0.6		0.3		0.3
MAY 24	550	460	420		550	890	880	920		890	0.6	0.5	0.5		0.6
MAY 25	380	190			50	1450	1450			1470	0.3	0.1			0
MAY 27	210	90			50	760	800			760	0.3	0.1			0.1
JUNE 21	150	80		110	50	410	390		460	430	0.4	0.2		0.2	0.1
JUNE 10		1290		1350	1290		1700		1820	1650		0.8		0.7	0.8
JULY 3		400		390			490		570			0.8		0.7	

.023 CYCLES PER MINUTE

JAN 10	860				410	1460				1540	0.6				0.3
MARCH 5	850		400		410	1670		1730		1590	0.5		0.2		0.3
MAY 24	580	450	350		450	860	880	930		820	0.7	0.5	0.4		0.6
MAY 25	460	360			460	1160	1160			1110	0.4	0.3			0.4
MAY 27	250	170			100	720	800			720	0.3	0.2			0.1
JUNE 21	220	170		140	170	320	300		360	340	0.7	0.6		0.4	0.5
JUNE 10		720		680	750		1180		1140	1070		0.6		0.6	0.7
JULY 3		330		340			450		470			0.7		0.7	

.025 CYCLES PER MINUTE

JAN 10	840				390	1390				1390	0.6				0.3
MARCH 5	580		240		240	1280		1300		1200	0.5		0.2		0.2
MAY 24	370	250	220		200	670	700	740		640	0.6	0.4	0.3		0.3
MAY 25	760	640			710	820	800			660	0.9	0.8			1.1
MAY 27	240	140			120	640	750			640	0.4	0.2			0.2
JUNE 21	250	210		160	220	270	250		300	280	0.9	0.9		0.5	0.8
JUNE 10		310		240	390		490		480	420		0.6		0.5	0.9
JULY 3		260		280			450		410			0.6		0.7	

Table 6 Comparison along the Profile of the Spectral Densities (in Gamma-minutes) Representing the Vertical Change Z and the Horizontal Change in an East-West Direction S together with the Ratio Z/S

APPENDIX I FOURIER ANALYSIS

1. A function f(t) can be expanded in any interval (-T,T) so long as it satisfies the Dirichlet condition in the interval and if $\int_{-\infty}^{+\infty} |f(t)|dt$ converges. The function may be developed in a Fourier Series

$$f(t) = \frac{a_0}{2} + \sum_{n=1}^{\infty} a_n \cos\frac{n\pi t}{T} + \sum_{n=1}^{\infty} b_n \sin\frac{n\pi t}{T}$$

where $-T \leq t < T$

and

$$a_0 = \frac{1}{T}\int_{-T}^{T} f(x)\,dx$$

$$a_n = \frac{1}{T}\int_{-T}^{T} f(x)\cos\frac{n\pi x}{T}\,dx$$

$$b_n = \frac{1}{T}\int_{-T}^{T} f(x)\sin\frac{n\pi x}{T}\,dx$$

Writing

$$\Delta\omega = \frac{\pi}{T},$$

$$f(t) = \frac{\Delta\omega}{2\pi}\int_{-T}^{+T} f(x)\,dx + \sum_{n=1}^{\infty}\frac{\Delta\omega}{\pi}\left[\int_{-T}^{+T} f(x)\cos n\Delta\omega x\,dx\cdot\cos n\Delta\omega t + \int_{-T}^{+T} f(x)\sin n\Delta\omega x\,dx\cdot\sin n\Delta\omega t\right]$$

The interval (-T,T) may be expanded to $(-\infty,\infty)$ by letting $T\to\infty$, so that $\Delta\omega\to 0$ and in the limit

$$f(t)\to\int_{-\infty}^{+\infty}\left\{\left[\frac{1}{2\pi}\int_{-\infty}^{+\infty} f(x)\cos\omega x\,dx\right]\cos\omega t + \left[\frac{1}{2\pi}\int_{-\infty}^{+\infty} f(x)\sin\omega x\,dx\right]\sin\omega t\right\}d\omega$$

The cosine and sine spectral densities $A(\omega)$ and $B(\omega)$ are

defined as follows:

$$A(\omega) = \frac{1}{2\pi} \int_{-\infty}^{+\infty} f(x) \cos \omega x \, dx$$

$$B(\omega) = \frac{1}{2\pi} \int_{-\infty}^{+\infty} f(x) \sin \omega x \, dx$$

so that

$$f(t) = \int_{-\infty}^{+\infty} \left[A(\omega) \cos \omega t + B(\omega) \sin \omega t \right] d\omega$$

2. The Fourier Series for f(t) may also be written in an exponential form

$$f(t) = \sum_{-\infty}^{+\infty} c_n e^{\frac{-in\pi t}{T}} \qquad \text{where} \qquad c_n = \frac{1}{2T} \int_{-T}^{+T} f(x) \, e^{\frac{+in\pi x}{T}} \, dx$$

As before this reduces to an integral form in the limit as $T \to \infty$ i.e.

$$f(t) = \int_{-\infty}^{+\infty} C(\omega) \, e^{-i\omega t} \, d\omega$$

where

$$C(\omega) = \frac{1}{2\pi} \int_{-\infty}^{+\infty} e^{i\omega x} f(x) \, dx$$

and

$$\left| C(\omega) \right| = \sqrt{\left(A(\omega) \right)^2 + \left(B(\omega) \right)^2}$$

Hence, f(t) may be synthesized by a sum of terms $e^{-i\omega t}$ covering all angular frequencies in the continuous infinite range $(-\infty, \infty)$. These terms have infinitesimal amplitudes given by the expression

$|C(\omega)|\,d\omega$. The amplitude density spectrum $|C(\omega)|$ is, therefore, not the actual amplitude characteristic of f(t), but rather a characteristic which shows relative magnitude only.

APPENDIX II MAGNETOGRAMS

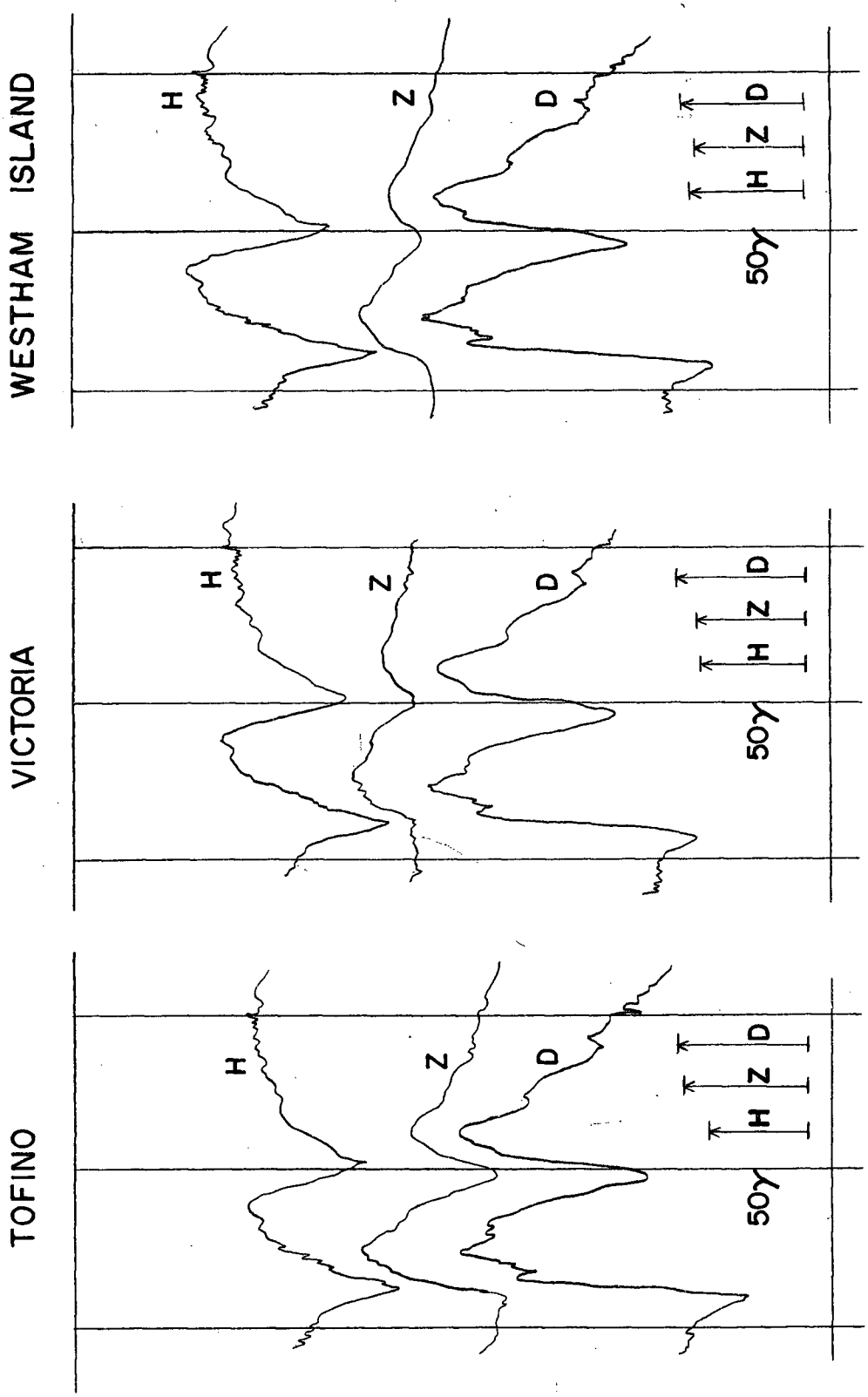

Recorded March 5, 1964 0100 to 0300 U.T.

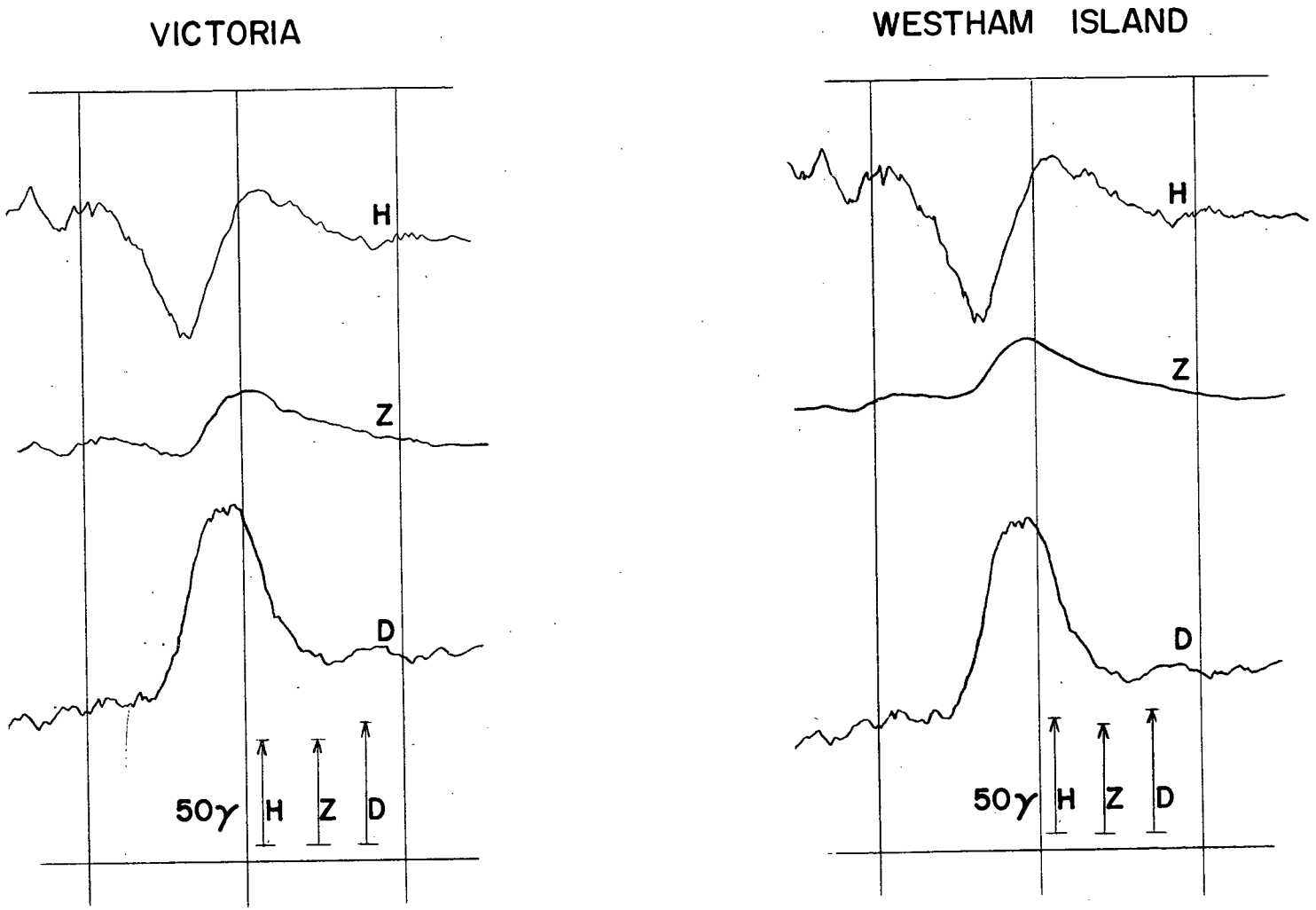

Recorded April 29, 1964 0100 to 0300 U.T.

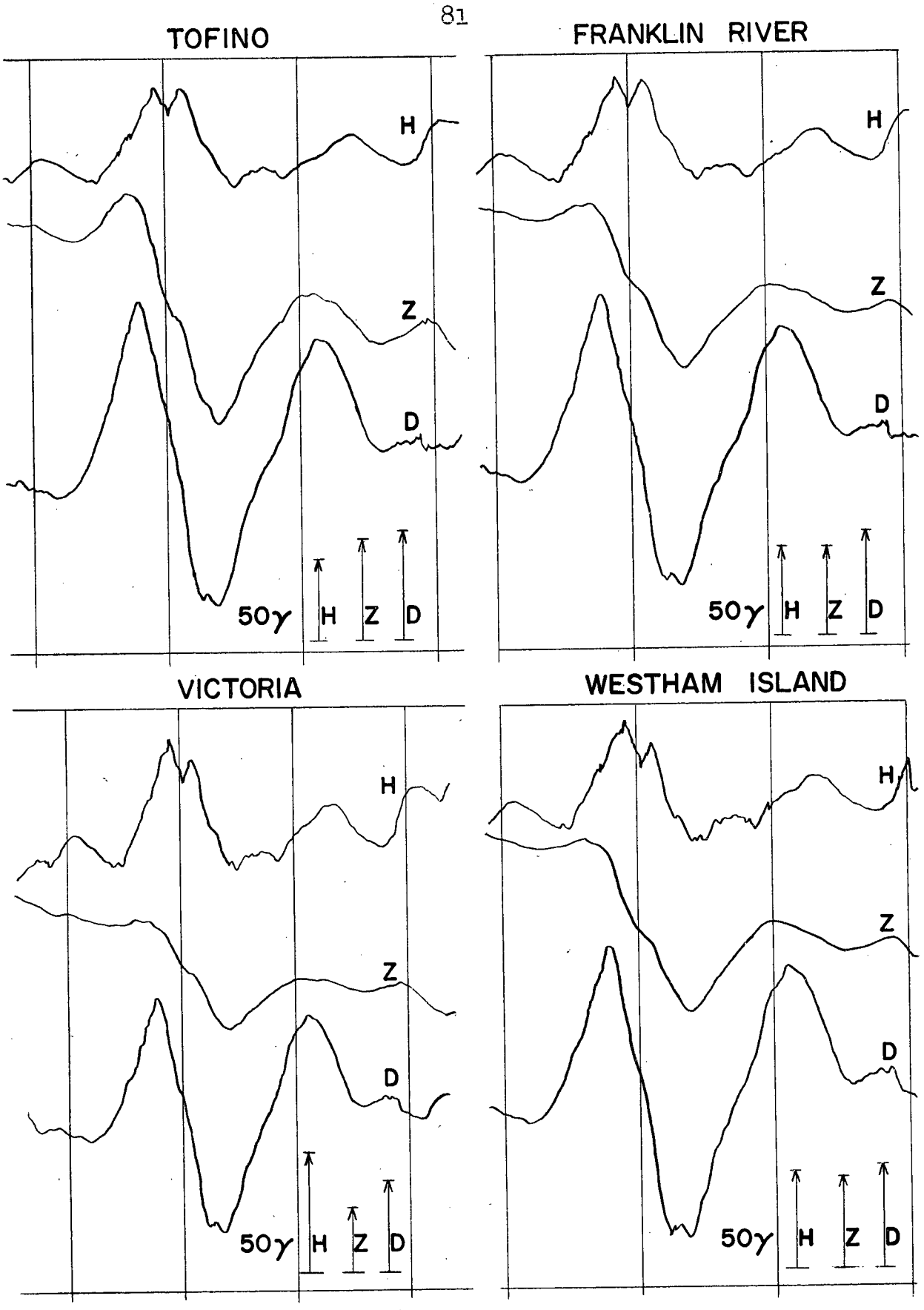

Recorded May 24, 1964 0600 to 0900 U.T.

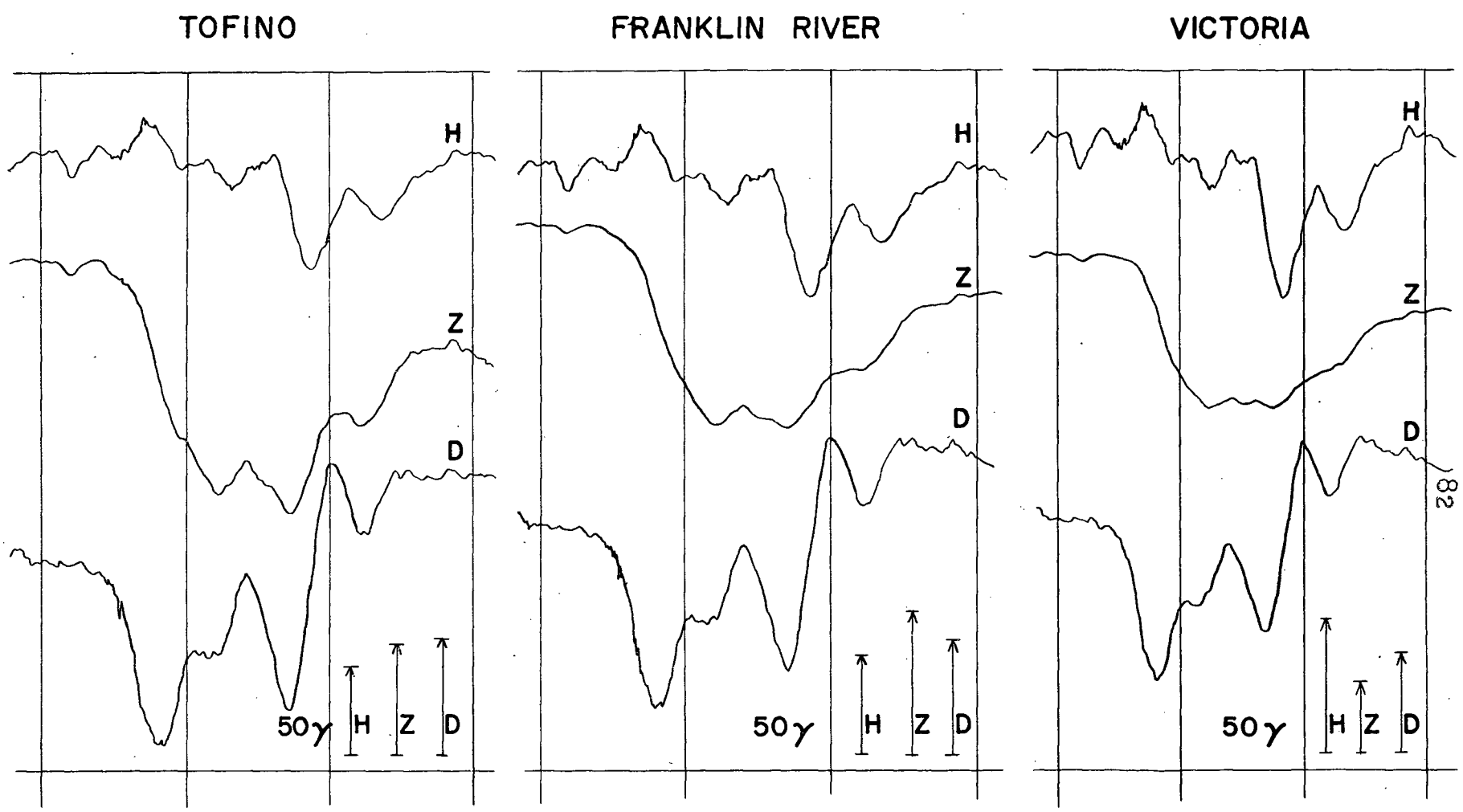

Recorded May 25, 1964 0800 to 1100 U.T.

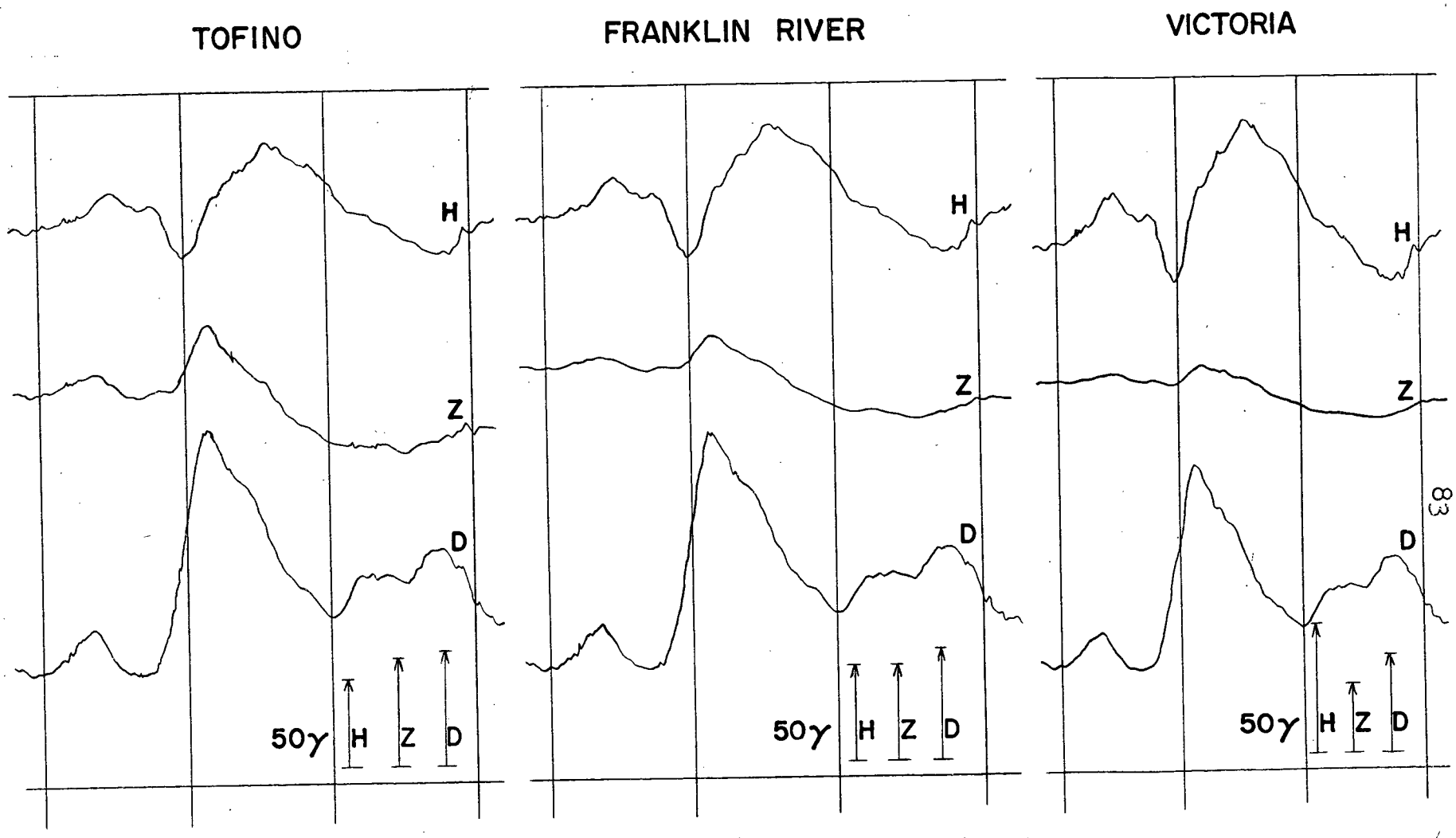

Recorded May 27, 1964 0700 to 1000 U.T.

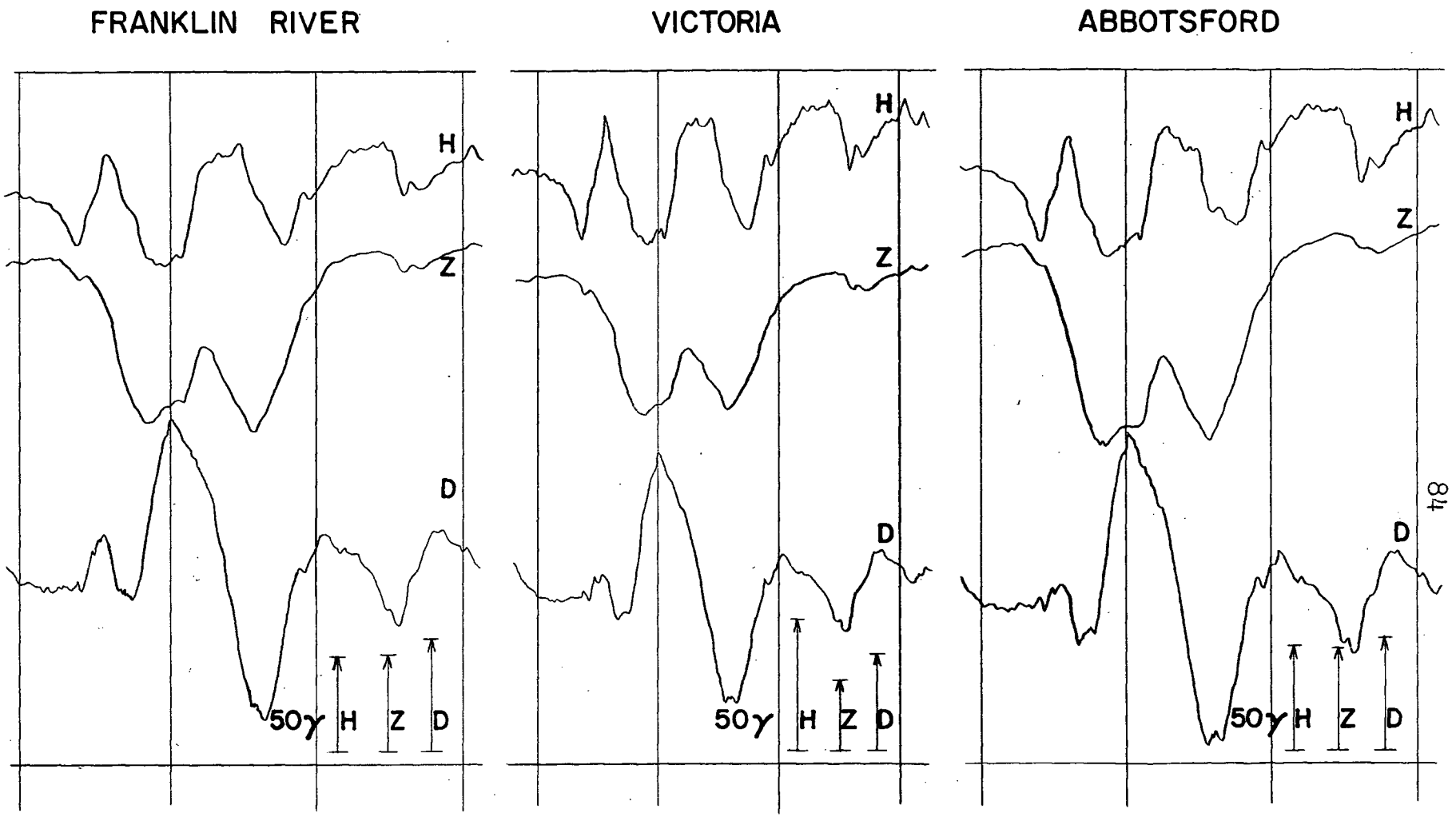

Recorded June 10, 1964 0900 to 1200 U.T.

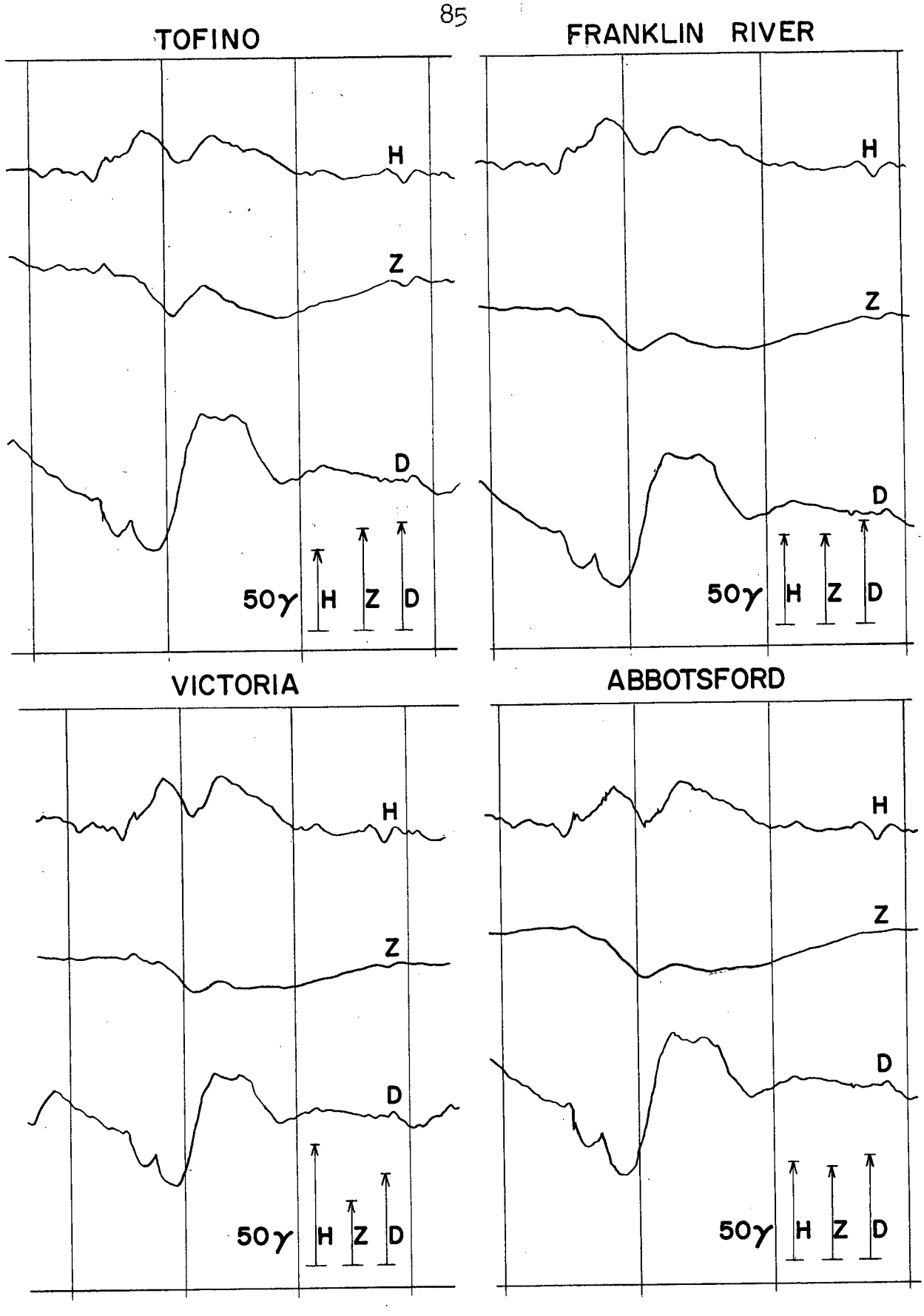

Recorded June 21, 1964 0800 to 1100 U.T.

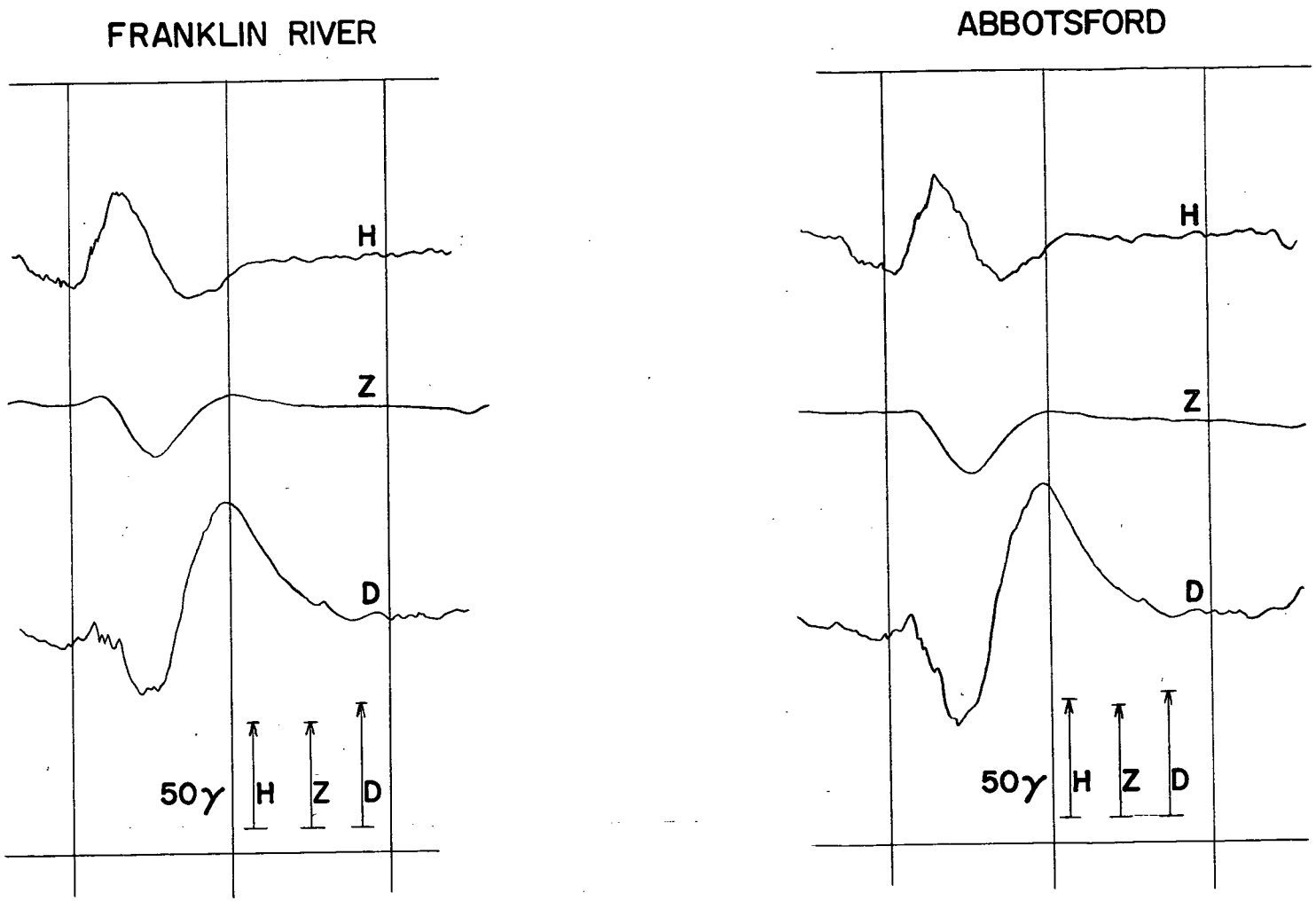

Recorded July 3, 1964 0700 to 0900 U.T.

REFERENCES

1. Ashour, A.A., The Induction of Electric Currents in a Uniform Circular Disk. Q.J. Mech. Appl. Math., 3, 119 (1950)

2. Brooks, C.E.P., N. Carruthers., Handbook of Statistical Methods in Meteorology. London: H.M.S.O. (1953)

3. Cagniard, L., Principles of the Magnetotelluric Method, a new Method of Geophysical Prospecting. Geophys., 18, 605 (1953)

4. Cantwell, T., Detection and Analysis of Low Frequency Magnetotelluric Signals. Ph.D. Thesis, Massachusetts Institute of Technology (1960)

5. Coode, A., Electric and Magnetic Fields Associated with a Vertical Fault. M.Sc. Thesis, University of British Columbia (1963)

6. Chapman, S., The Solar and Lunar Variations of the Earth's Magnetism. Phil. Trans. Roy. Soc. Lond. A218, 1 (1919)

7. Chapman, S., T.T. Whitehead, The Influence of Electrically Conducting Material within the Earth on Various Phenomena of Terrestrial Magnetism. Trans. Camb. Phil. Soc., 22, 463 (1922)

8. Chapman, S., A.T. Price, The Electric and Magnetic State of the Interior of the Earth, as Inferred from Terrestrial Magnetic Variations. Phil. Trans. Roy. Soc. Lond. A229, 427, (1930)

9. Chapman, S., T. Bartels, Geomagnetism, vols. 1 and 2, Oxford University Press (1940)

10. Christoffel, D.A., J.A. Jacobs, E.J. Jolley, J.K. Kinnear, J.A. Shand, The Fraser Delta Experiment of 1960. P.N.L. Lab Rept. 61-5, D.R.B. Canada (1961)

11. D'Erceville, J., G. Kunetz, The Effect of a Fault on the Earth's Natural Electromagnetic Field. Geophys., 27, 651, (1962)

12. Dietz, R.S., Continent and Ocean Basin Evolution by Spreading of the Sea Floor. Nature, 190, 855 (1961)

13. Dorman, J., M. Ewing, J. Oliver, Study of Shear-velocity Distribution in the Upper Mantle by Mantle Rayleigh Waves. Bull. Seis. Soc. Am., 50, 87 (1960)

14. Gutenberg, B., The Low-Velocity Layers in the Earth's Mantle. Geol. Soc. Am. Spec. Paper 65, 337 (1954)

15. Hess, H.H., Geological Hypotheses and the Earth's Crust under the Oceans. Proc. Roy. Soc. Lond. A, 222, 341 (1954)

16. Hyndman, R.D., Electrical Conductivity Inhomogeneities in the Earth's Upper Mantle. M.Sc. Thesis, University of British Columbia (1963)

17. Jacobs, J.A., Continental Drift. Nature, 185, 231 (1960)

18. Lahiri, B.N., A.T. Price, Electromagnetic Induction within a Non-Uniform Earth. Phil. Trans. Roy. Soc. Lond. A, 237, 509 (1939)

19. Mansurov, S.M., On Some Peculiarities of the Variable Geomagnetic Field in the Region of the South Pole Observatory Mirny. Ann. I.G.Y., Pergamon Press, 11, 104 (1961)

20. Mason,C.S., M.N. Hill, Diurnal Variations of the Earth's Magnetic Field at Sea. Nature, 195, 365 (1962)

21. Nagata, T., T. Oguti, H. Maekawa, Model Experiments of Electromagnetic Induction within the Earth. Bull. Earth Res. Inst., 33, 561 (1955)

22. Niblett, E.R., C. Sayn-Wittgenstein, Variations of Electrical Conductivity with Depth by the Magnetotelluric Method. Geophys., 25, 998 (1960)

23. Parkinson, W.D., Direction of Rapid Geomagnetic Fluctuations. Geophys. J., 2, 1 (1959)

24. Parkinson, W.D., The Influence of Continents and Oceans on Geomagnetic Variations. Geophys. J., 6, 441 (1962)

25. Parkinson, W.D., Conductivity Anomalies in Australia and the Ocean Effect. J. Geomag. Geoele., 15, 222 (1964)

26. Ponomarev, Ye. A., The Nature of the Geomagnetic Coast Effect. "Geomagnetic Disturbances", Academy of Sciences Press, Moscow (1960) (translated by E.R. Hope, D.R.B., Canada, Publ. T382R (1963))

27. Price, A.T., Electromagnetic Induction in a Uniform Permeable Conducting Sphere. Proc. Lond. Math. Soc. Ser. 2, 33, 233 (1931)

28. Price, A.T., The Induction of Electric Currents in Non-Uniform Thin Sheets and Shells. Q. J. Mech. Appl. Math., 2, 283 (1949)

29. Price, A.T., Electromagnetic Induction in a Uniform Semi-Infinite Conductor. Q. J. Mech. and Appl. Math., 3, 385 (1950)

30. Price, A.T., The Theory of Magnetotelluric Methods when the Source Field is Considered. J. Geophys. Res., 67, 1907 (1962)

31. Price, A.T., A note on the Interpretation of Magnetic Variations and Magnetotelluric Data. J. Geomag. Geoele., 15, 241 (1964)

32. Rankin, D., The Magnetotelluric Effect of a Dike. Geophys. 27, 667 (1962)

33. Rikitake, T., Electromagnetic Induction within the Earth and its Relation to the Electrical State of the Earth's Interior. Bull. Earth. Res. Inst., 28, 45 and 219 (1950); 29, 61 and 539 (1951)

34. Rikitake, T., I. Yokayama, The Anomalous Behaviour of Geomagnetic Variations of Short Period in Japan and Its Relation to the Subterranean Structure. The 6th Report. Bull. Earth Res. Inst., 33, 297 (1955)

35. Rikitake, T., Anomaly of Geomagnetic Variations in Japan. Geophys. J., 2, 276 (1959)

36. Rikitake, T., The Effect of the Ocean on Rapid Geomagnetic Changes. Geophys. J., 5, 1 (1961)

37. Rikitake, T., Sq and Ocean. J. Geophys. Res., 66, 3245 (1961)

38. Rikitake, T., The Possibility of Detecting the Mantle Low Velocity Layer by Geomagnetic Deep Sounding. Bull. Earth. Res. Inst., 40, 495 (1962)

39. Rikitake, T., A Possible Cause of Earth-Current Anisotropy. Bull. Earth. Res. Inst., 40, 685 (1962)

40. Rikitake, T., T. Yabu, K. Yamakawa, The Anomalous Behaviour of Geomagnetic Variations of Short Period in Japan and Its Relation to the Subterranean Structure. The 10th Report. Bull. Earth. Res. Inst., 40, 693 (1962)

41. Rikitake,T., Outline of the Anomaly of Geomagnetic Variations in Japan. J. Geomag. Geoele., 15, 181 (1964)

42. Roden, R.B., The Effect of an Ocean on Magnetic Diurnal Variations. Geophys. J., 8, 375 (1964)

43. Rokitjansky, I.I., P.K. Senko, S.M. Mansurov, J.K. Kalinin, G.A. Fonarev, The Coast Effect in the Variations of the Earth's Electromagnetic Field. J. Geomag. Geoele., 15, 271, (1964)

44. Rostoker, G., Low Frequency Variations in the Earth's Magnetic Field and Their Relation to the Conductivity of the Upper Mantle. M.A. Thesis, University of Toronto (1963)

45. Schmucker, U., Erdmagnetische Tiefensondierung in Deutschland 1957/59: Magnetogramme und Erste Auswertung. Abh. Akad. Wiss. in Goettingen, Math-phys. Kl. Beit. Inter. Geophy. Jahr Heft 5 (1959)

46. Schmucker, U., Annual Progress Report, Deep Anomalies in Electrical Conductivity. S.I.O. Ref. 61-13, Scripps Inst. of Oceanography (1960)

47. Schmucker, U., Anomalies of Geomagnetic Variations in the Southwestern United States. J. Geomagn. Geoele., 15, 193 (1964)

48. Siebert, M., W. Kertz, Zur Zerlegung eines lokalen erdmagnetischen Feldes in Ausseren und innernen Anteil. Nachr. Akad. Wiss. Goettingen, Math-Phys. Kl. Abt., IIa, 87 (1957)

49. Simeon, G., A. Sposito, Anomalies in Geomagnetic Variations in Italy. J. Geomag. Geoele., 15, 249 (1964)

50. Srivastava, S., J. Douglas, S. Ward, The Application of the Magnetotelluric and Telluric Methods in Central Alberta. Geophys., 28, 426 (1963)

51. Stratton, J.A., Electromagnetic Theory. McGraw Hill, New York-London (1941)

52. Man'yan, L.L., Ye. P. Kharin, Some Laws Exhibited by Geomagnetic Bays in the Middle Latitudes. Geology and Geophysics (U.S.S.R. Acad Sciences, Siberian Division), 9, 125-129 (1963) (translated by E.R. Hope, D.R.B., Canada, Publ. T404R (1964))

53. Von Herzen, R.P., S. Uyeda, Heat Flow through the Eastern Pacific Ocean Floor. J. Geophys. Res., 68, 4219 (1963)

54. Wait, J., On the Relation between Telluric Currents and the Earth's Magnetic Field. Geophys., 19, 281 (1954)

55. Weaver, J., A Note on the Vertical Fault Problem in Magnetotelluric Theory. Tech. Mem. 62-1, P.N.L., D.R.B., Canada (1962)

56. Weaver, J., The Electromagnetic Field Within a Discontinuous Conductor with Reference to Geomagnetic Micropulsations near a Coastline. Can. J. Phys., 41, 484 (1963)

57. Weaver, J., On the Separation of Local Geomagnetic Fields into External and Internal Parts. Zeits. Geophys., 30, 29 (1964)

58. White, W.R.H., J.C. Savage, A Seismic and Gravity Study of the Earth's Crust in British Columbia. Bull. Seis. Soc. Am., (in press 1965)

59. Whitham, K., F. Anderson, The Anomaly in Geomagnetic Variations at Alert in the Arctic Archipelago of Canada. Geophys. J., 7, 220 (1962)

60. Whitham, K., Anomalies in Geomagnetic Variations in the Arctic Archipelago of Canada. J. Geomag. Geoele, 15, 227 (1964)

61. Zhigalov, L.N., Some Features of the Variations of the Geomagnetic Vertical Component in the Arctic Ocean. "Geomagnetic Disturbances", Academy of Sciences Press, Moscow, (1960) (translated by E.R. Hope, D.R.B., Canada, Publ. T358R (1961))